INDEPENDENT JOURNAL OF MANAGEMENT & PRODUCTION (IJM&P)
http://www.ijmp.jor.br v. 12, n. 9, Special Edition, December 21, IFLOG 2020
ISSN: 2236-269X
DOI: 10.14807/ijmp.v12i9.1554

STUDY OF FORCES IN A 2T9R ROBOT MECHANISM

Adriana Comanescu
IFToMM, Romania
E-mail: adrianacomanescu@yahoo.com

Alexandra Rotaru
IFToMM, Romania
E-mail: alexandra.rotaru11@gmail.com

Florian Ion Tiberiu Petrescu
IFToMM, Romania
E-mail: fitpetrescu@gmail.com

Submission: 1/18/2021
Accept: 1/20/2021

ABSTRACT

The paper presents in detail a method of calculating the forces acting on a 2T9R type robot. In order to determine the reactions (forces in the kinematic couples), one must first determine the inertial forces in the mechanism to which one or more useful loads of the robot can be added. The torsor of the inertia forces is calculated with the help of the masses of the machine elements and the accelerations from the centers of mass of the mechanism elements, so the positions, velocities, and accelerations acting on it will be determined, i.e. its complete kinematics. The calculation method applied by a MathCad program intelligently uses data entry through the IFLOG logic function so that the calculations can be automated. So the effective automation of the calculation program is done exclusively through the IFLOG functions originally used in the paper.

Keywords: IFLOG; Robot; 2T9R robot; Forces; Kinematics; Geometric-analytical method; Direct kinematics; Inverse kinematics

http://www.ijmp.jor.br v. 12, n. 9, Special Edition, December 21, IFLOG 2020
ISSN: 2236-269X
DOI: 10.14807/ijmp.v12i9.1554

1. INTRODUCTION

Robots have always fascinated us, but today we use them massively, in almost all industrial areas, especially where they work hard, repetitive and tiring, in toxic, chemical, radioactive environments, underwater, in the cosmos, in dangerous environments, on mined lands, in hard to reach areas, etc. It can be said once again that, just as software and microchips have helped us to quickly write various useful programs and implement them directly, so robotics has made our daily work much easier.

Thanks to robots, automation is almost perfect today, product quality is very high, the manufacturing price has dropped a lot, you can work in continuous fire, people have escaped hard work, tiring, repetitive, in toxic environments and now can treat other problems more important, such as design, scientific research, to work only 5 days a week with high income and, in the future, due to the massive implementation of increasingly modern robots with increased capabilities, man will reach the work week only 4 days.

An even greater increase is expected in the number of specialized robots implemented in large factories and factories around the world.

Due to the massive use of industrial robots, the diversification in this field has gained high levels. For this reason, we want to study in this paper a new robot model, 2T9R, extremely complex in movements, useful in any type of work, a versatile robot, which can weld, cut, process different parts, to assemble them, or to manipulate them from one working strip to another, and in the same way, he can also paint the different machined components before their assembly.

The robot has various advantages due to its complex mode arranged since the design and will be able to easily adapt to any type of automated manufacturing cell. For this reason, and because it is an original one and has not been studied before, we want that in this paper we review its study completely with the determination of all the forces that act it and that appear within it, the one that it also requires a complete kinematic calculation (Antonescu & Petrescu, 1985; 1989; Antonescu *et al*., 1985a; 1985b; 1986; 1987; 1988; 1994; 1997; 2000a; 2000b; 2001; Atefi et al., 2008; Avaei et al., 2008; Aversa *et al*., 2017a; 2017b; 2017c; 2017d; 2017e; 2016a; 2016b; 2016c; 2016d; 2016e; 2016f; 2016g; 2016h; 2016i; 2016j; 2016k; 2016l; 2016m; 2016n; 2016o; Azaga; Othman, 2008; Cao *et al*., 2013; Dong *et al*., 2013; El-Tous, 2008; Comanescu, 2010; Franklin, 1930; He *et al*., 2013; Jolgaf et al., 2008; Kannappan et al., 2008; Lee, 2013; Lin *et al*., 2013; Liu *et al*., 2013; Meena & Rittidech, 2008; Meena et al., 2008; Mirsayar *et al*., 2017; Ng et al., 2008; Padula, Perdereau &

ISSN: 2236-269X
DOI: 10.14807/ijmp.v12i9.1554

Pannirselvam, 2008; 2013; Perumaal & Jawahar, 2013; Petrescu, 2011; 2015a; 2015b; Petrescu & Petrescu, 1995a; 1995b; 1997a; 1997b; 1997c; 2000a; 2000b; 2002a; 2002b; 2003; 2005a; 2005b; 2005c; 2005d; 2005e; 2011a; 2011b; 2012a; 2012b; 2013a; 2013b; 2016a; 2016b; 2016c; Petrescu *et al.*, 2009; 2016; 2017a; 2017b; 2017c; 2017d; 2017e; 2017f; 2017g; 2017h; 2017i; 2017j; 2017k; 2017l; 2017m; 2017n; 2017o; 2017p; 2017q; 2017r; 2017s; 2017t; 2017u; 2017v; 2017w; 2017x; 2017y; 2017z; 2017aa; 2017ab; 2017ac; 2017ad; 2017ae; 2018a; 2018b; 2018c; 2018d; 2018e; 2018f; 2018g; 2018h; 2018i; 2018j; 2018k; 2018l; 2018m; 2018n; Pourmahmoud, 2008; Rajasekaran et al., 2008; Shojaeefard et al., 2008; Taher et al., 2008; Tavallaei & Tousi, 2008; Theansuwan & Triratanasirichai, 2008; Zahedi et al., 2008; Zulkifli et al., 2008).

2. METHODS AND MATERIALS

The present study will start with a description of the 2T9R robot proposed to be analyzed, in terms of the forces acting on it. The 2T9R mechanism (Figure 1) has a constructive model based on a bimobile kinematic chain having three independent contours (Figure 2a) obtained from the bicontour chain of the 2T6R mechanism.

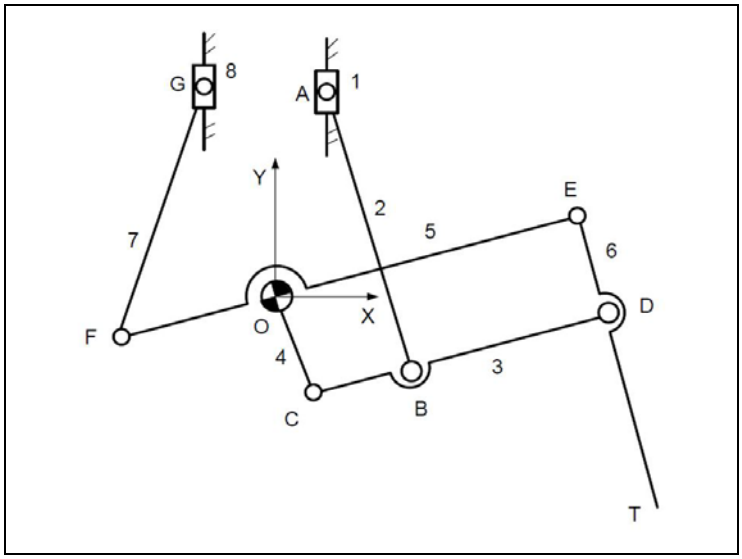

Figure 1: The mechanism 2T9R

The direct structural model (Figure 2b) consists of two initial active modular groups GMAI (A, 1) and GMAI (G, 8) which constitute the linear motors that drive it and two passive modular groups, one of the type of the GMP2 triad (2, 3,4,6) and the other of the GMP1 dyad type (5,7). The connection of the modular groups for the direct model is shown in Figure 3.

ISSN: 2236-269X
DOI: 10.14807/ijmp.v12i9.1554

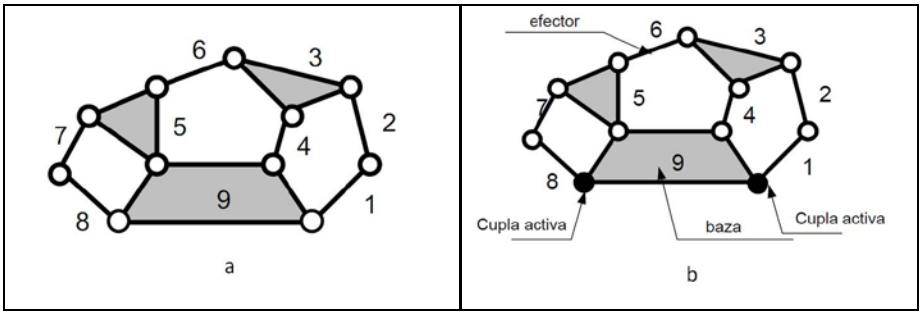

Figure 2: Structural scheme of the mechanism

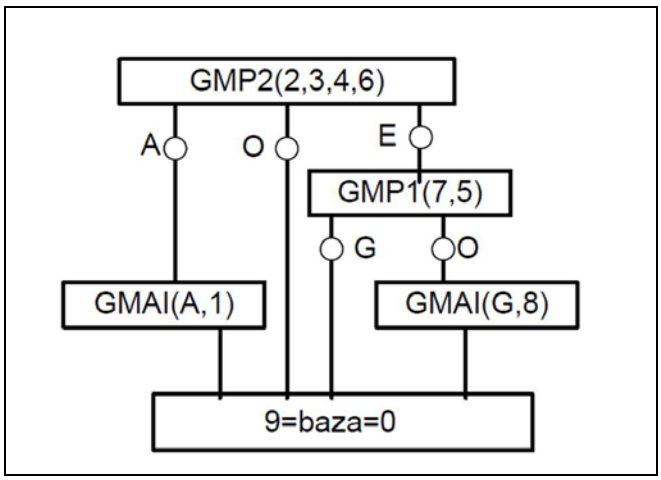

Figure 3: Electronic or wiring diagram (block diagram) of the mechanism

The direct structural model (Figure 2b) and the connection of the corresponding modular groups (Figure 3) are used to determine the reaction torsor in each kinematic coupling using the kinetostatic principle.

To study the main plane mechanism of the 2T9R robot, its kinematic elements, kinematic torques, and positioning angles of the elements that also have rotation are initially established (Figure 4).

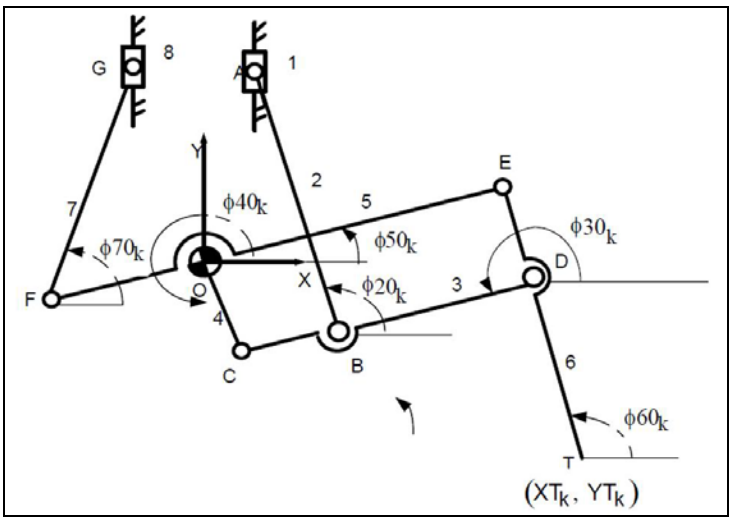

Figure 4: Determining the kinematic elements, the kinematic torques, and the angles that position the elements that also have a rotation

http://www.ijmp.jor.br v. 12, n. 9, Special Edition, December 21, IFLOG 2020
ISSN: 2236-269X
DOI: 10.14807/ijmp.v12i9.1554

For the kinetostatic analysis (determination of the forces in the mechanism) the centers of mass marked with the letter T (Figure 5) are positioned as follows: O ≡ T5 ≡ T4; B ≡ T2 ≡ T3; E ≡ T6; F ≡ T7. Their placement does not influence the algorithm for calculating the components of the reaction torsion in the kinematic torques.

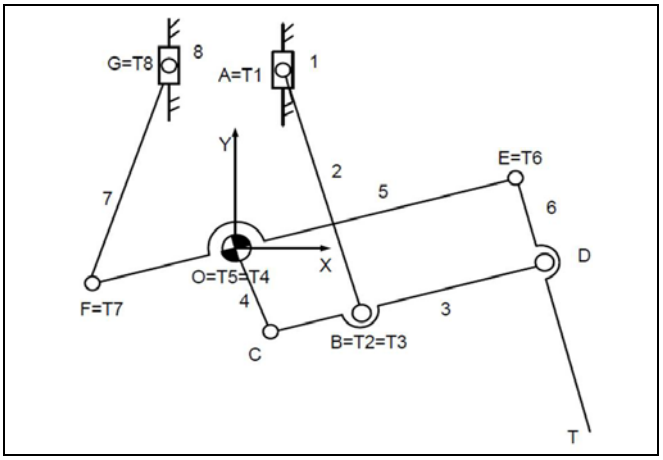

Figure 5: Positioning the centers of mass T of all the elements of the mechanism

It is considered a single external force RT acting on the system neglecting other external forces (for example - gravitational forces). This simplification brings some peculiarities in the form of terms from the calculation algorithm without restricting its generality. The forces of weight are not recommended to be introduced in the sizing calculations because their influence is sometimes by addition and sometimes by decrease it being therefore opposite and having negative effects on the sizing of a mechanism. On the other hand, in large (large) robots, if they still work fast (at high speeds), the inertial forces (internal forces, which arise even in the mechanism due to its masses) are considerable and much higher than those weights that automatically become negligible.

2.1. Determination of Reactions in the kinematic torques of the triad (2,3,4,6)

The study of forces is always processed inversely to the kinematic one, ie not from the motors to the final effector element, but inversely, from the modular group furthest from the motors to them. For this reason, the force calculations start on the triad (2,3,4,6) from Figure 6.

INDEPENDENT JOURNAL OF MANAGEMENT & PRODUCTION (IJM&P)
http://www.ijmp.jor.br v. 12, n. 9, Special Edition, December 21, IFLOG 2020
ISSN: 2236-269X
DOI: 10.14807/ijmp.v12i9.1554

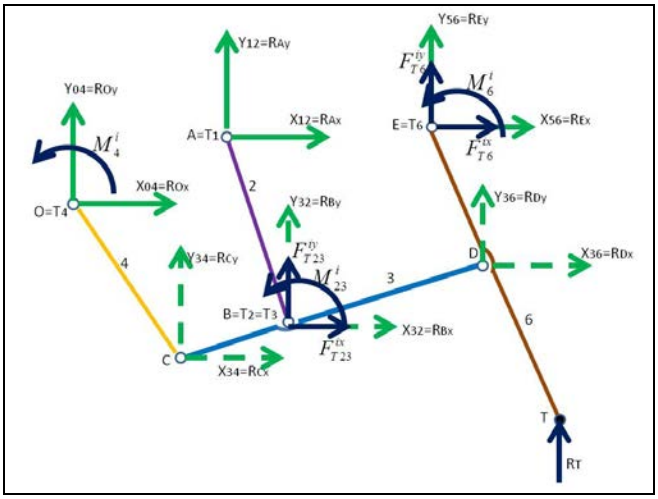

Figure 6: The forces on the triad (2,3,4,6). The known forces are shown in blue; the reactions (unknown forces in the kinematic couplings) are drawn in green.

To determine the unknown forces, the reactions (from the kinematic couplings), the following calculation relations are written (from 2 ROx is made explicit, from 3 RAx, which is introduced in relation 1 and I is obtained, and in relation 4 and II is obtained, where I and II represent two linear equations with two unknowns that make up a linear system that can be solved immediately by Kramer III):

$$\begin{cases} \sum M_E^{Tr} = 0 \\ M_4^i + R_O^x \cdot (y_E - y_O) - R_O^y \cdot (x_E - x_O) + R_A^x \cdot (y_E - y_A) - R_A^y \cdot (x_E - x_A) + \\ M_6^i + M_{23}^i + F_{T23}^{ix} \cdot (y_E - y_B) - F_{T23}^{iy} \cdot (x_E - x_B) + R_T \cdot (x_T - x_E) = 0 \end{cases} \quad (1)$$

$$\begin{cases} \sum M_C^{(4)} = 0 \\ M_4^i - R_O^x \cdot (y_O - y_C) - R_O^y \cdot (x_C - x_O) = 0 \end{cases} \quad (2)$$

$$\begin{cases} \sum M_B^{(2)} = 0 \\ M_2^i - R_A^x \cdot (y_A - y_B) - R_A^y \cdot (x_B - x_A) = 0 \end{cases} \quad (3)$$

$$\begin{cases} \sum M_D^{(4,3,2)} = 0 \\ M_4^i + M_{23}^i + R_O^x \cdot (y_D - y_O) - R_O^y \cdot (x_D - x_O) - R_A^x \cdot (y_A - y_D) - R_A^y \cdot (x_D - x_A) + \\ F_{T23}^{ix} \cdot (y_D - y_B) - F_{T23}^{iy} \cdot (x_D - x_B) = 0 \end{cases} \quad (4)$$

$$\begin{cases} \sum F_x^{(4,3,2,6)} = 0 \\ R_O^x + R_A^x + R_E^x + F_{T23}^{ix} + F_{T6}^{ix} = 0 \end{cases} \quad (5)$$

$$\begin{cases} \sum F_y^{(4,3,2,6)} = 0 \\ R_O^y + R_A^y + R_E^y + F_{T23}^{iy} + F_{T6}^{iy} + R_T = 0 \end{cases} \quad (6)$$

INDEPENDENT JOURNAL OF MANAGEMENT & PRODUCTION (IJM&P)
http://www.ijmp.jor.br v. 12, n. 9, Special Edition, December 21, IFLOG 2020
ISSN: 2236-269X
DOI: 10.14807/ijmp.v12i9.1554

$$\begin{cases} R_O^y \cdot \left[(x_O - x_E) + \dfrac{(x_O - x_C)\cdot(y_E - y_O)}{(y_O - y_C)} \right] + R_A^y \cdot \left[(x_A - x_E) + \dfrac{(x_A - x_B)\cdot(y_E - y_A)}{(y_A - y_B)} \right] \\ = M_4^i \dfrac{(y_O - y_E)}{(y_O - y_C)} + M_2^i \dfrac{(y_A - y_E)}{(y_A - y_B)} - M_4^i - M_6^i - M_{23}^i + F_{T23}^{ix} \cdot (y_B - y_E) + \\ F_{T23}^{iy} \cdot (x_E - x_B) + R_T \cdot (x_E - x_T) \end{cases} \quad \text{(I)}$$

$$\begin{cases} R_O^y \cdot \left[(x_O - x_D) + \dfrac{(x_O - x_C)\cdot(y_D - y_O)}{(y_O - y_C)} \right] + R_A^y \cdot \left[(x_A - x_D) + \dfrac{(x_A - x_B)\cdot(y_D - y_A)}{(y_A - y_B)} \right] \\ = M_4^i \dfrac{(y_O - y_D)}{(y_O - y_C)} + M_2^i \dfrac{(y_A - y_D)}{(y_A - y_B)} - M_4^i - M_{23}^i + F_{T23}^{ix} \cdot (y_B - y_D) + F_{T23}^{iy} \cdot (x_D - x_B) \end{cases} \quad \text{(II)}$$

$$\begin{cases} \begin{cases} a_{11} \cdot R_O^y + a_{12} \cdot R_A^y = a_1 \\ a_{21} \cdot R_O^y + a_{22} \cdot R_A^y = a_2 \end{cases} \\ a_{11} = (x_O - x_E) + \dfrac{(x_O - x_C)\cdot(y_E - y_O)}{(y_O - y_C)} \\ a_{12} = (x_A - x_E) + \dfrac{(x_A - x_B)\cdot(y_E - y_A)}{(y_A - y_B)} \\ a_1 = M_4^i \dfrac{(y_O - y_E)}{(y_O - y_C)} + M_2^i \dfrac{(y_A - y_E)}{(y_A - y_B)} - M_4^i - M_6^i - M_{23}^i + F_{T23}^{ix} \cdot (y_B - y_E) + \\ F_{T23}^{iy} \cdot (x_E - x_B) + R_T \cdot (x_E - x_T) \\ \\ a_{21} = (x_O - x_D) + \dfrac{(x_O - x_C)\cdot(y_D - y_O)}{(y_O - y_C)} \\ a_{22} = (x_A - x_D) + \dfrac{(x_A - x_B)\cdot(y_D - y_A)}{(y_A - y_B)} \\ a_2 = M_4^i \dfrac{(y_O - y_D)}{(y_O - y_C)} + M_2^i \dfrac{(y_A - y_D)}{(y_A - y_B)} - M_4^i - M_{23}^i + F_{T23}^{ix} \cdot (y_B - y_D) + F_{T23}^{iy} \cdot (x_D - x_B) \\ \Delta = \begin{vmatrix} a_{11} & a_{12} \\ a_{21} & a_{22} \end{vmatrix} = a_{11} \cdot a_{22} - a_{12} \cdot a_{21} \quad \Delta_O = \begin{vmatrix} a_1 & a_{12} \\ a_2 & a_{22} \end{vmatrix} = a_1 \cdot a_{22} - a_{12} \cdot a_2 \\ \Delta_A = \begin{vmatrix} a_{11} & a_1 \\ a_{21} & a_2 \end{vmatrix} = a_{11} \cdot a_2 - a_1 \cdot a_{21} \quad R_O^y = \dfrac{\Delta_O}{\Delta}; \quad R_A^y = \dfrac{\Delta_A}{\Delta} \end{cases} \quad \text{(III)}$$

With (IV) on determines R_{Ox} si R_{Ax}:

ISSN: 2236-269X
DOI: 10.14807/ijmp.v12i9.1554

$$\begin{cases} R_O^x = \dfrac{M_4^i + R_O^y \cdot (x_O - x_C)}{(y_O - y_C)} \\ R_A^x = \dfrac{M_2^i + R_A^y \cdot (x_A - x_B)}{(y_A - y_B)} \end{cases} \quad \text{(IV)}$$

From (5) results relation (V) which determines R_{Ex}, and from (6) results the expression (VI) which generates R_{Ey}:

$$R_E^x = -\left(R_O^x + R_A^x + F_{T23}^{ix} + F_{T6}^{ix}\right) \quad \text{(V)}$$

$$R_E^y = -\left(R_O^y + R_A^y + F_{T23}^{iy} + F_{T6}^{iy} + R_T\right) \quad \text{(VI)}$$

Can now write the next equations (7-15):

$$\sum F_x^{(4)} = 0 \Rightarrow R_C^x \equiv X_{34} = -\left(R_O^x\right) \Rightarrow X_{43} = -X_{34} = R_O^x \quad (7)$$

$$\sum F_y^{(4)} = 0 \Rightarrow R_C^y \equiv Y_{34} = -\left(R_O^y\right) \Rightarrow Y_{43} = -Y_{34} = R_O^y \quad (8)$$

$$\sum F_x^{(2)} = 0 \Rightarrow R_B^x \equiv X_{32} = -\left(R_A^x + F_{T2}^{ix}\right) \Rightarrow X_{23} = -X_{32} \quad (9)$$

$$\sum F_y^{(2)} = 0 \Rightarrow R_B^y \equiv Y_{32} = -\left(R_A^y + F_{T2}^{iy}\right) \Rightarrow Y_{23} = -Y_{32} \quad (10)$$

$$\sum F_x^{(6)} = 0 \Rightarrow R_D^x \equiv X_{36} = -\left(R_E^x + F_{T6}^{ix}\right) \Rightarrow X_{63} = -X_{36} \quad (11)$$

$$\sum F_y^{(6)} = 0 \Rightarrow R_D^y \equiv Y_{36} = -\left(R_E^y + F_{T6}^{iy} + R_T\right) \Rightarrow Y_{63} = -Y_{36} \quad (12)$$

$$X_{40} = -X_{04} = -R_O^x; \quad Y_{40} = -Y_{04} = -R_O^y \quad (13)$$

In order to perform the triad calculations (2,3,4,6) it is necessary to present briefly the expressions by which the known inertial forces, inside the mechanism, due to the masses of the component elements (16-20) are determined by calculations:

$$M_4^i = -J_{T_4} \cdot \varepsilon_4 = -J_O^{(4)} \cdot \varepsilon_4 \quad (16)$$

$$\begin{cases} F_{T_2}^{ix} = -m_2 \cdot \ddot{x}_B \\ F_{T_2}^{iy} = -m_2 \cdot \ddot{y}_B \\ M_2^i = -J_B^{(2)} \cdot \varepsilon_2 \end{cases} \quad (17)$$

$$\begin{cases} F_{T_3}^{ix} = -m_3 \cdot \ddot{x}_B \\ F_{T_3}^{iy} = -m_3 \cdot \ddot{y}_B \\ M_3^i = -J_B^{(3)} \cdot \varepsilon_3 \end{cases} \quad (18)$$

ISSN: 2236-269X
DOI: 10.14807/ijmp.v12i9.1554

$$\begin{cases} F_{T_{23}}^{ix} = F_{T_2}^{ix} + F_{T_3}^{ix} = -(m_2 + m_3) \cdot \ddot{x}_B \\ F_{T_{23}}^{iy} = F_{T_2}^{iy} + F_{T_3}^{iy} = -(m_2 + m_3) \cdot \ddot{y}_B \\ M_{23}^{i} = M_2^{i} + M_3^{i} = -J_B^{(2)} \cdot \varepsilon_2 - J_B^{(3)} \cdot \varepsilon_3 \end{cases} \quad (19)$$

$$\begin{cases} F_{T_6}^{ix} = -m_6 \cdot \ddot{x}_E \\ F_{T_6}^{iy} = -m_6 \cdot \ddot{y}_E \\ M_6^{i} = -J_E^{(6)} \cdot \varepsilon_6 \end{cases} \quad (20)$$

2.2. Determination of Reactions in the kinematic couplings of the dyad (5,7)

Dyad 5.7 has the following charges (Figure 7), where the already known forces are shown in blue, and the unknown ones in green, i.e. the reactions in the kinematic torques of the dyad, which will be determined.

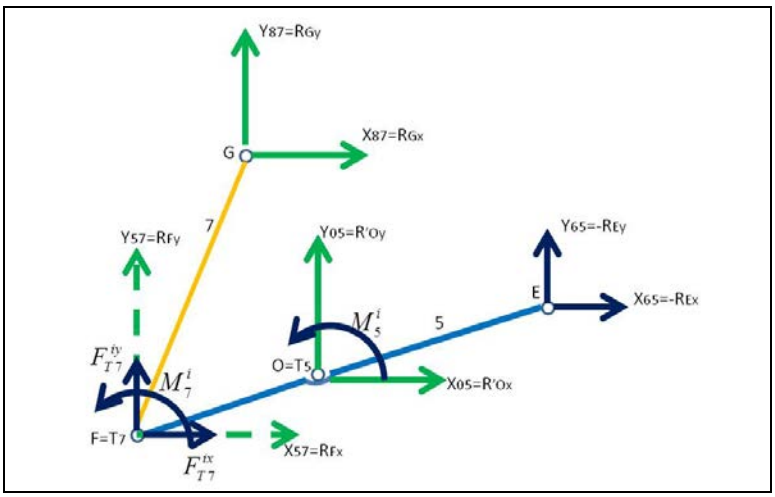

Figure 7: Forces of the dyad 5-7

Can write the relations 21-22:

$$\begin{cases} \sum M_O^{(7,5)} = 0 \\ M_7^{i} + M_5^{i} - R_G^{x} \cdot (y_G - y_O) - R_G^{y} \cdot (x_O - x_G) + F_{T7}^{ix} \cdot (y_O - y_F) - F_{T7}^{iy} \cdot (x_O - x_F) \\ - X_{65} \cdot (y_E - y_O) + Y_{65} \cdot (x_E - x_O) = 0 \end{cases} \quad (21)$$

$$\begin{cases} \sum M_F^{(7)} = 0 \\ M_7^{i} - R_G^{x} \cdot (y_G - y_F) + R_G^{y} \cdot (x_G - x_F) = 0 \end{cases} \quad (22)$$

From relation (22) one explicitly reaction R_{Gy} (24) which is introduced in relation (21) obtaining directly the value R_{Gx} (23), and then R_{Gy} (24):

ISSN: 2236-269X
DOI: 10.14807/ijmp.v12i9.1554

$$R_G^x = \frac{F_{T7}^{ix}(y_F - y_O) + F_{T7}^{iy}(x_O - x_F) + R_E^x(y_O - y_E) + R_E^y(x_E - x_O) - M_7^i - M_5^i + M_7^i \frac{(x_G - x_O)}{(x_G - x_F)}}{\frac{(y_O - y_G)\cdot(x_G - x_F) + (y_G - y_F)\cdot(x_G - x_O)}{(x_G - x_F)}} \tag{23}$$

$$R_G^y = \frac{R_G^x(y_G - y_F) - M_7^i}{(x_G - x_F)} \Rightarrow Y_{78} = -Y_{87} = -R_G^y \tag{24}$$

Now, one write the relations (25-30):

$$\sum F_x^{(7)} = 0 \Rightarrow R_F^x \equiv X_{57} = -\left(R_G^x + F_{T7}^{ix}\right) \Rightarrow X_{75} = -X_{57} \tag{25}$$

$$\sum F_y^{(7)} = 0 \Rightarrow R_F^y \equiv Y_{57} = -\left(R_G^y + F_{T7}^{iy}\right) \Rightarrow Y_{75} = -Y_{57} \tag{26}$$

$$\sum F_x^{(5)} = 0 \Rightarrow X_{05} = -\left(X_{65} + X_{75}\right) = R_E^x + R_F^x \tag{27}$$

$$\sum F_y^{(5)} = 0 \Rightarrow Y_{05} = -\left(Y_{65} + Y_{75}\right) = R_E^y + R_F^y \tag{28}$$

$$X_{50} \equiv -R'^x_O = -X_{05} = -(R_E^x + R_F^x) \tag{29}$$

$$Y_{50} \equiv -R'^y_O = -Y_{05} = -(R_E^y + R_F^y) \tag{30}$$

The torsor of the inertial forces on dyad 5,7 is determined by the relations (31-32):

$$M_5^i = -J_O^{(5)} \cdot \varepsilon_5 \tag{31}$$

$$\begin{cases} F_{T_7}^{ix} = -m_7 \cdot \ddot{x}_F \\ F_{T_7}^{iy} = -m_7 \cdot \ddot{y}_F \\ M_7^i = -J_F^{(7)} \cdot \varepsilon_7 \end{cases} \tag{32}$$

2.3. Determination of the reactions in the kinematic torques of the motor element 8 and calculation of the driving force Fm8

Figure 8 shows all the forces acting on the linear motor element 8, in the rotation torque G (between elements 8 and 7) and in the translation torque T8 (between elements 8 and 0) materialized by the guideline between the motor piston 8 and its axis of vertical symmetry coinciding with the guide 0, considering as the point of actuation of the forces 08 the center of mass T8. The forces in the torque are the x-axis and y-axis projections of the already known R78 reaction (thus shown in dark blue).

INDEPENDENT JOURNAL OF MANAGEMENT & PRODUCTION (IJM&P)
http://www.ijmp.jor.br v. 12, n. 9, Special Edition, December 21, IFLOG 2020
ISSN: 2236-269X
DOI: 10.14807/ijmp.v12i9.1554

Also known the torsion of the inertial forces on element 8, represented here only by an inertial force along the guide axis y (its action being concentrated in the center of mass T8), there is no movement on the x-axis acceleration and automatic and force inertial on this x-axis is canceled, and the inertial moment is also canceled permanently because there is no rotational motion, the angular and automatic acceleration and the inertial moment being canceled.

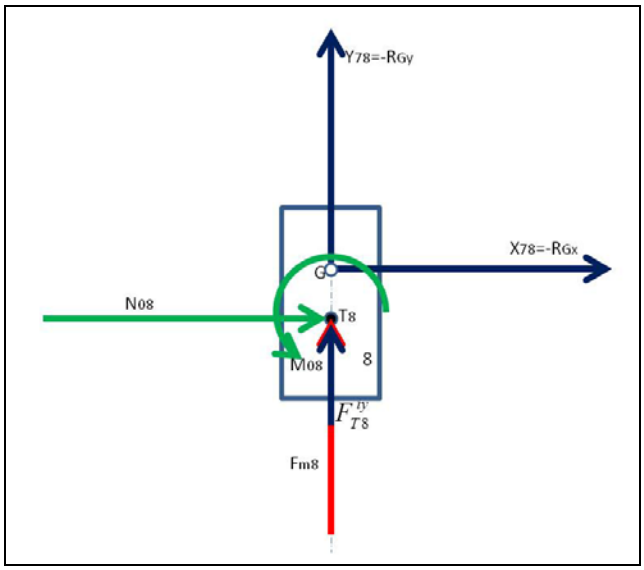

Figure 8: Forces acting on the engine element 8

The driving force that moves the linear motor element 8 also acts in the center of mass. Practically except for the reaction in coupling G all other forces act on the center of mass T8. Relationships can be written (33-36):

$$F_{T_8}^{\dot{I}y} = -m_8 \cdot \ddot{y}_G \tag{33}$$

$$\sum F_x^{(8)} = 0 \Rightarrow X_{78} + N_{08} = 0 \Rightarrow N_{08} = -X_{78} \Rightarrow N_{08} = R_G^x \tag{34}$$

$$\sum F_y^{(8)} = 0 \Rightarrow F_{m8} + Y_{78} + F_{T_8}^{\dot{I}y} = 0 \Rightarrow F_{m8} = -Y_{78} - F_{T_8}^{\dot{I}y} \Rightarrow F_{m8} = R_G^y - F_{T_8}^{\dot{I}y} \tag{35}$$

$$\sum M_{T_8}^{(8)} = 0 \Rightarrow M_{08} - X_{78} \cdot \left(y_G - y_{T_8}\right) = 0 \Rightarrow M_{08} = R_G^x \cdot \left(y_{T_8} - y_G\right) \tag{36}$$

It is specified here that if the points G and T8 coincide the moment M08 is canceled together with the phase shift ($\left(y_{T_8} - y_G\right)$=0).

The procedure is then repeated for engine 1 (Figure 9, relations 37-40).

ISSN: 2236-269X
DOI: 10.14807/ijmp.v12i9.1554

2.4. Determination of the reactions in the kinematic torques of the motor element 1 and calculation of the driving force Fm1

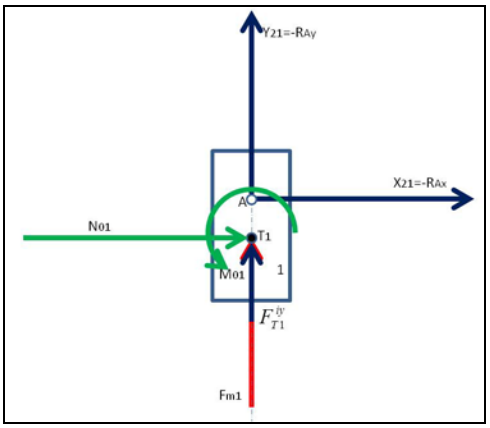

Figure 9: Forces acting on the engine element 1

$$F_{T_1}^{\dot{y}} = -m_1 \cdot \ddot{y}_A \tag{37}$$

$$\sum F_x^{(1)} = 0 \Rightarrow X_{21} + N_{01} = 0 \Rightarrow N_{01} = -X_{21} \Rightarrow N_{01} = R_A^x \tag{38}$$

$$\sum F_y^{(1)} = 0 \Rightarrow F_{m1} + Y_{21} + F_{T_1}^{\dot{y}} = 0 \Rightarrow F_{m1} = -Y_{21} - F_{T_1}^{\dot{y}} \Rightarrow F_{m1} = R_A^y - F_{T_1}^{\dot{y}} \tag{39}$$

$$\sum M_{T_1}^{(1)} = 0 \Rightarrow M_{01} - X_{21} \cdot \left(y_A - y_{T_1}\right) = 0 \Rightarrow M_{01} = R_A^x \cdot \left(y_{T_1} - y_A\right) \tag{40}$$

It is specified that if points A and T1 coincide the moment M01 is canceled together with the phase shift ($\left(y_{T_1} - y_A\right)$=0).

Remarks: Any torque introduces a reaction that decomposes along the coordinate axes (in the plane) into two components along the x and y axes, while each translation torque introduces a reaction perpendicular to the torque guide axis and a moment.

Any reaction in any pair is easily determined by having the modulus (size) given by the radical in the sum of the squares of the two scalar components of the reaction, and its position (the direction of the vector defining it) is given by an alpha angle measured from the horizontal which passes through the origin of the reaction (the respective coupling) and which has the trigonometric functions described by the two-component scalar and the vector of the respective reaction.

2.5. Determination of robot speeds and accelerations

The kinematic calculation of the robot's speeds and accelerations is done only by direct kinematics as it is operated in reality, while the positions can be determined in two distinct situations, by direct kinematics when we are interested in the normal operation of the robot, finding the workspace. and the trajectories described by the effector element (or other

ISSN: 2236-269X
DOI: 10.14807/ijmp.v12i9.1554

component kinematic couplings), or by using inverse kinematics when the positions that the final element (effector) must occupy successively are already imposed and the successive positions of the driving elements must be determined, for this robot the linear motors 1 and 8.

2.6. Determination of robot speeds and accelerations to the dyad 5,7

As stated, only direct kinematics is used to determine speeds and accelerations, so the calculations from dyad 5.7 are started (Figure 10).

Write the calculation relationships in the system (41):

The scalar coordinates, velocities, and accelerations of points G and O are known, with the help of which, using the equations of the two circles formed, the scalar coordinates of point F are determined. Then easily determine the angles FI5 and FI7 with their derivatives, ω_5,ε_5, ω_7,ε_7.

$$\begin{cases} (x_G-x_F)^2+(y_G-y_F)^2=i^2 \Rightarrow 2(x_G-x_F)\cdot(\dot{x}_G-\dot{x}_F)+2(y_G-y_F)\cdot(\dot{y}_G-\dot{y}_F)=0 \\ (x_F-x_O)^2+(y_F-y_O)^2=f^2; x_O=y_O=0 \Rightarrow 2x_F\cdot\dot{x}_F+2y_F\cdot\dot{y}_F \Rightarrow \dot{y}_F=-\dfrac{x_F\dot{x}_F}{y_F} \\ \dot{x}_F=\dfrac{(y_G-y_F)\cdot y_F\cdot\dot{y}_G}{(x_G-x_F)\cdot y_F-(y_G-y_F)\cdot x_F}; \omega_7=\dfrac{\dot{y}_G-\dot{y}_F}{x_G-x_F}; \varepsilon_7=\dfrac{\ddot{y}_G-\ddot{y}_F-\omega_7(\dot{x}_G-\dot{x}_F)}{x_G-x_F} \\ \dot{y}_F=\dfrac{-(y_G-y_F)\cdot x_F\cdot\dot{y}_G}{(x_G-x_F)\cdot y_F-(y_G-y_F)\cdot x_F} \Rightarrow \omega_5=\dfrac{\dot{y}_F}{x_F} \Rightarrow \varepsilon_5=\dfrac{\ddot{y}_F-\omega_5\cdot\dot{x}_F}{x_F} \\ \ddot{x}_F=\dfrac{(\dot{y}_G-\dot{y}_F)\cdot y_F\cdot\dot{y}_G+(y_G-y_F)\cdot\dot{y}_F\cdot\dot{y}_G+(y_G-y_F)\cdot y_F\cdot\ddot{y}_G}{(x_G-x_F)\cdot y_F-(y_G-y_F)\cdot x_F}- \\ \dfrac{\dot{x}_F[(\dot{x}_G-\dot{x}_F)\cdot y_F-(\dot{y}_G-\dot{y}_F)\cdot x_F+(x_G-x_F)\cdot\dot{y}_F-(y_G-y_F)\cdot\dot{x}_F]}{(x_G-x_F)\cdot y_F-(y_G-y_F)\cdot x_F} \\ \ddot{y}_F=\dfrac{-\dot{x}_F^2-\dot{y}_F^2-x_F\cdot\ddot{x}_F}{y_F} \\ x_E=e\cdot\cos\varphi_5 \Rightarrow \dot{x}_E=-e\cdot\sin\varphi_5\cdot\omega_5 \Rightarrow \ddot{x}_E=-e\cdot\cos\varphi_5\cdot\omega_5^2-e\cdot\sin\varphi_5\cdot\varepsilon_5 \\ y_E=e\cdot\sin\varphi_5 \Rightarrow \dot{y}_E=e\cdot\cos\varphi_5\cdot\omega_5 \Rightarrow \ddot{y}_E=-e\cdot\sin\varphi_5\cdot\omega_5^2+e\cdot\cos\varphi_5\cdot\varepsilon_5 \end{cases} \quad (41)$$

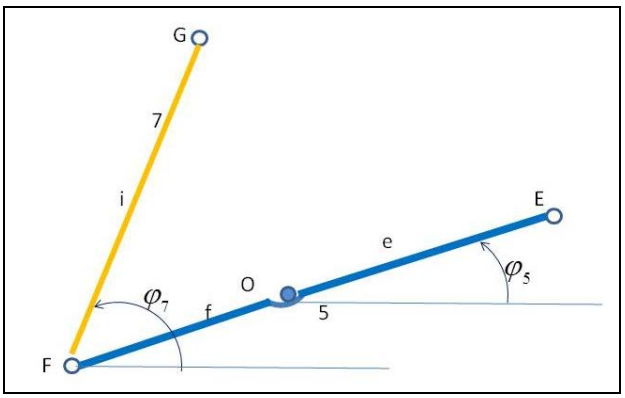

Figure 10: Direct kinematics on dyad 5.7: speeds and accelerations

ISSN: 2236-269X
DOI: 10.14807/ijmp.v12i9.1554

2.7. Determination of speeds and accelerations in the triad 2,3,4,6

In figure 11 you can see the positions with the sizes characteristic of triad 2,3,4,6 starting from which the relations of positions, speeds, and accelerations are written.

Position relations being considered already solved and all known position values (solved separately by direct or inverse kinematics as required), derived directly twice and thus obtaining triad speeds and accelerations (2,3,4,6), equations (42-52).

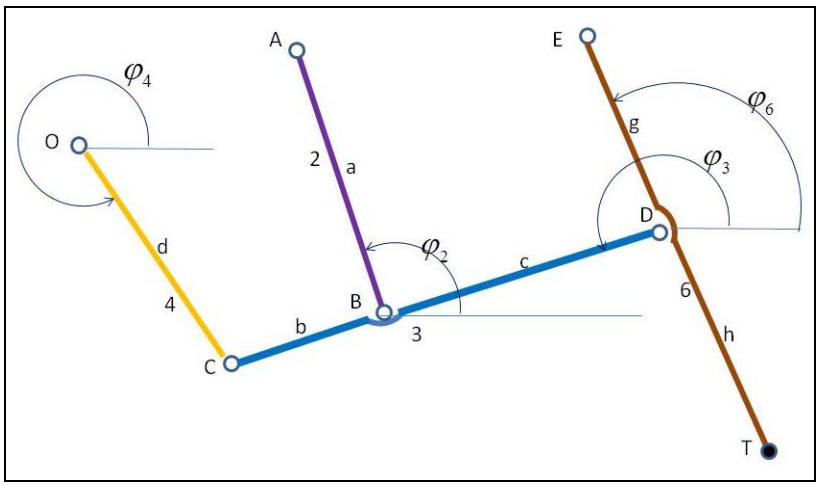

Figure 11: Kinematics of the triad 2,3,4,6

$$
\begin{cases}
\begin{cases} x_C = d\cdot\cos\varphi_4 \\ y_C = d\cdot\sin\varphi_4 \end{cases}
\begin{cases} \dot{x}_C = -d\cdot\sin\varphi_4\cdot\omega_4 \\ \dot{y}_C = d\cdot\cos\varphi_4\cdot\omega_4 \end{cases}
\begin{cases} x_B = x_A - a\cdot\cos\varphi_2 \\ y_B = y_A - a\cdot\sin\varphi_2 \end{cases}
\begin{cases} \dot{x}_B = \dot{x}_A + a\cdot\sin\varphi_2\cdot\omega_2 \\ \dot{y}_B = \dot{y}_A - a\cdot\cos\varphi_2\cdot\omega_2 \end{cases} \\
\begin{cases} x_C = x_B + b\cos\varphi_3 \\ y_C = y_B + b\sin\varphi_3 \end{cases}
\begin{cases} \dot{x}_C = \dot{x}_B - b\sin\varphi_3\omega_3 \\ \dot{y}_C = \dot{y}_B + b\cos\varphi_3\omega_3 \end{cases}
\begin{cases} -d\sin\varphi_4\omega_4 = \dot{x}_A + a\sin\varphi_2\omega_2 - b\sin\varphi_3\omega_3 \\ d\cos\varphi_4\omega_4 = \dot{y}_A - a\cos\varphi_2\omega_2 + b\cos\varphi_3\omega_3 \end{cases} \\
\\
\begin{cases} x_D = x_B - c\cos\varphi_3 \\ y_D = y_B - c\sin\varphi_3 \end{cases}
\begin{cases} \dot{x}_D = \dot{x}_B + c\sin\varphi_3\omega_3 \\ \dot{y}_D = \dot{y}_B - c\cos\varphi_3\omega_3 \end{cases}
\begin{cases} x_E = x_D + g\cos\varphi_6 \\ y_E = y_D + g\sin\varphi_6 \end{cases}
\begin{cases} \dot{x}_E = \dot{x}_D - g\sin\varphi_6\omega_6 \\ \dot{y}_E = \dot{y}_D + g\cos\varphi_6\omega_6 \end{cases} \\
\begin{cases} \dot{x}_A - \dot{x}_E + a\cdot\sin\varphi_2\cdot\omega_2 + c\cdot\sin\varphi_3\cdot\omega_3 = g\cdot\sin\varphi_6\cdot\omega_6 \\ \dot{y}_A - \dot{y}_E - a\cdot\cos\varphi_2\cdot\omega_2 - c\cdot\cos\varphi_3\cdot\omega_3 = -g\cdot\cos\varphi_6\cdot\omega_6 \end{cases}
\end{cases}
\tag{42}
$$

INDEPENDENT JOURNAL OF MANAGEMENT & PRODUCTION (IJM&P)
http://www.ijmp.jor.br v. 12, n. 9, Special Edition, December 21, IFLOG 2020
ISSN: 2236-269X
DOI: 10.14807/ijmp.v12i9.1554

$$\begin{cases} \begin{cases} -d\cdot\sin\varphi_4\cdot\omega_4 = \dot{x}_A + a\cdot\sin\varphi_2\cdot\omega_2 - b\cdot\sin\varphi_3\cdot\omega_3 \,|\cdot\cos\varphi_4 \\ d\cdot\cos\varphi_4\cdot\omega_4 = \dot{y}_A - a\cdot\cos\varphi_2\cdot\omega_2 + b\cdot\cos\varphi_3\cdot\omega_3 \,|\cdot\sin\varphi_4 \end{cases} \Rightarrow I \\ \\ \begin{cases} \dot{x}_A - \dot{x}_E + a\cdot\sin\varphi_2\cdot\omega_2 + c\cdot\sin\varphi_3\cdot\omega_3 = g\cdot\sin\varphi_6\cdot\omega_6 \,|\cdot\cos\varphi_6 \\ \dot{y}_A - \dot{y}_E - a\cdot\cos\varphi_2\cdot\omega_2 - c\cdot\cos\varphi_3\cdot\omega_3 = -g\cdot\cos\varphi_6\cdot\omega_6 \,|\cdot\sin\varphi_6 \end{cases} \Rightarrow II \\ \\ \begin{cases} (I): \dot{x}_A\cdot\cos\varphi_4 + \dot{y}_A\cdot\sin\varphi_4 + a\cdot\omega_2\cdot\sin(\varphi_2-\varphi_4) + b\cdot\omega_3\cdot\sin(\varphi_4-\varphi_3) = 0 \\ (II): (\dot{x}_A - \dot{x}_E)\cos\varphi_6 + (\dot{y}_A - \dot{y}_E)\sin\varphi_6 + a\omega_2\sin(\varphi_2-\varphi_6) + c\omega_3\sin(\varphi_3-\varphi_6) = 0 \end{cases} \end{cases} \tag{43}$$

$$\begin{cases} \begin{cases} \dot{x}_A\cdot\cos\varphi_4 + \dot{y}_A\cdot\sin\varphi_4 + a\cdot\omega_2\cdot\sin(\varphi_2-\varphi_4) + b\cdot\omega_3\cdot\sin(\varphi_4-\varphi_3) = 0 \\ (\dot{x}_A - \dot{x}_E)\cos\varphi_6 + (\dot{y}_A - \dot{y}_E)\sin\varphi_6 + a\omega_2\sin(\varphi_2-\varphi_6) + c\omega_3\sin(\varphi_3-\varphi_6) = 0 \end{cases} \\ (I)\cdot[c\cdot\sin(\varphi_3-\varphi_6)] \quad (II)\cdot[-b\cdot\sin(\varphi_4-\varphi_3)] \Rightarrow \omega_2 \\ (I)\cdot[\sin(\varphi_2-\varphi_6)] \quad (II)\cdot[-\sin(\varphi_2-\varphi_4)] \Rightarrow \omega_3 \\ \omega_2 = \dfrac{b[(\dot{x}_A - \dot{x}_E)\cos\varphi_6 + (\dot{y}_A - \dot{y}_E)\sin\varphi_6]\sin(\varphi_3-\varphi_4) + c(\dot{x}_A\cos\varphi_4 + \dot{y}_A\sin\varphi_4)\sin(\varphi_3-\varphi_6)}{a\cdot[c\cdot\sin(\varphi_2-\varphi_4)\cdot\sin(\varphi_6-\varphi_3) + b\cdot\sin(\varphi_2-\varphi_6)\cdot\sin(\varphi_4-\varphi_3)]} \\ \omega_3 = \dfrac{[(\dot{x}_A - \dot{x}_E)\cos\varphi_6 + (\dot{y}_A - \dot{y}_E)\sin\varphi_6]\sin(\varphi_2-\varphi_4) + (\dot{x}_A\cos\varphi_4 + \dot{y}_A\sin\varphi_4)\sin(\varphi_6-\varphi_2)}{[c\cdot\sin(\varphi_2-\varphi_4)\cdot\sin(\varphi_6-\varphi_3) + b\cdot\sin(\varphi_2-\varphi_6)\cdot\sin(\varphi_4-\varphi_3)]} \\ \\ \omega_4 = \dfrac{\dot{y}_A - \dot{x}_A - a\cdot\omega_2\cdot\cos(\varphi_4-\varphi_2) + b\cdot\omega_3\cdot\cos(\varphi_4-\varphi_3)}{d} \\ \omega_6 = \dfrac{\dot{x}_A - \dot{x}_E + \dot{y}_E - \dot{y}_A + a\cdot\omega_2\cdot\cos(\varphi_6-\varphi_2) + c\cdot\omega_3\cdot\cos(\varphi_6-\varphi_3)}{g} \\ \begin{cases} \dot{x}_C = -d\sin\varphi_4\omega_4 \\ \dot{y}_C = d\cos\varphi_4\omega_4 \end{cases} \begin{cases} \dot{x}_B = \dot{x}_A + a\sin\varphi_2\omega_2 \\ \dot{y}_B = \dot{y}_A - a\cos\varphi_2\omega_2 \end{cases} \begin{cases} \dot{x}_D = \dot{x}_B + c\sin\varphi_3\omega_3 \\ \dot{y}_D = \dot{y}_B - c\cos\varphi_3\omega_3 \end{cases} \begin{cases} \dot{x}_T = \dot{x}_D + h\sin\varphi_6\omega_6 \\ \dot{y}_T = \dot{y}_D - h\cos\varphi_6\omega_6 \end{cases} \end{cases} \tag{44}$$

$$\begin{cases} \varepsilon_2\cdot[ac\sin(\varphi_2-\varphi_4)\sin(\varphi_6-\varphi_3) + ab\sin(\varphi_2-\varphi_6)\sin(\varphi_4-\varphi_3)] = \\ = \omega_2\cdot[ac\cos(\varphi_2-\varphi_4)\sin(\varphi_3-\varphi_6)(\omega_2-\omega_4) + ac\sin(\varphi_4-\varphi_2)\cos(\varphi_6-\varphi_3)(\omega_6-\omega_3) + \\ ab\cos(\varphi_2-\varphi_6)\sin(\varphi_3-\varphi_4)(\omega_2-\omega_6) + ab\sin(\varphi_6-\varphi_2)\cos(\varphi_4-\varphi_3)(\omega_4-\omega_3)] + \\ [(\ddot{x}_A - \ddot{x}_E)\cos\varphi_6 + (\dot{x}_E - \dot{x}_A)\sin\varphi_6\omega_6 + (\ddot{y}_A - \ddot{y}_E)\sin\varphi_6 + (\dot{y}_A - \dot{y}_E)\cos\varphi_6\omega_6]b\sin(\varphi_3-\varphi_4) + \\ [(\dot{x}_A - \dot{x}_E)\cos\varphi_6 + (\dot{y}_A - \dot{y}_E)\sin\varphi_6]b\cos(\varphi_3-\varphi_4)(\omega_3-\omega_4) + (\ddot{x}_A\cos\varphi_4 + \ddot{y}_A\sin\varphi_4 - \\ \dot{x}_A\sin\varphi_4\omega_4 + \dot{y}_A\cos\varphi_4\omega_4)c\sin(\varphi_3-\varphi_6) + (\dot{x}_A\cos\varphi_4 + \dot{y}_A\sin\varphi_4)c\cos(\varphi_3-\varphi_6)(\omega_3-\omega_6) \end{cases} \tag{45}$$

ISSN: 2236-269X
DOI: 10.14807/ijmp.v12i9.1554

$$\begin{cases}\varepsilon_3 \cdot [b\sin(\varphi_4-\varphi_3)\sin(\varphi_2-\varphi_6)+c\sin(\varphi_3-\varphi_6)\sin(\varphi_4-\varphi_2)]= \\ =\omega_3 \cdot [b\cos(\varphi_4-\varphi_3)\sin(\varphi_6-\varphi_2)(\omega_4-\omega_3)+b\sin(\varphi_3-\varphi_4)\cos(\varphi_2-\varphi_6)(\omega_2-\omega_6)+ \\ c\cos(\varphi_3-\varphi_6)\sin(\varphi_2-\varphi_4)(\omega_3-\omega_6)+c\sin(\varphi_6-\varphi_3)\cos(\varphi_4-\varphi_2)(\omega_4-\omega_2)]+ \\ (\ddot{x}_A\cos\varphi_4+\ddot{y}_A\sin\varphi_4-\dot{x}_A\sin\varphi_4\omega_4+\dot{y}_A\cos\varphi_4\omega_4)\sin(\varphi_6-\varphi_2)+ \\ (\dot{x}_A\cos\varphi_4+\dot{y}_A\sin\varphi_4)\cos(\varphi_6-\varphi_2)(\omega_6-\omega_2)+\sin(\varphi_2-\varphi_4)\cdot[(\ddot{x}_A-\ddot{x}_E)\cos\varphi_6+ \\ (\ddot{y}_A-\ddot{y}_E)\sin\varphi_6+(\dot{x}_E-\dot{x}_A)\sin\varphi_6\omega_6+(\dot{y}_A-\dot{y}_E)\cos\varphi_6\omega_6]+ \\ [(\dot{x}_A-\dot{x}_E)\cos\varphi_6+(\dot{y}_A-\dot{y}_E)\sin\varphi_6]\cdot\cos(\varphi_2-\varphi_4)(\omega_2-\omega_4)\end{cases} \quad (46)$$

$$\begin{cases}\varepsilon_4 \cdot d= \\ =(\ddot{y}_A+a\sin\varphi_2\omega_2^2-a\cos\varphi_2\varepsilon_2-b\sin\varphi_3\omega_3^2+b\cos\varphi_3\varepsilon_3)\cos\varphi_4- \\ (\dot{y}_A-a\cos\varphi_2\omega_2+b\cos\varphi_3\omega_3)\sin\varphi_4\omega_4-\sin\varphi_4(\ddot{x}_A+a\cos\varphi_2\omega_2^2+a\sin\varphi_2\varepsilon_2- \\ b\cos\varphi_3\omega_3^2-b\sin\varphi_3\varepsilon_3)-(\dot{x}_A+a\sin\varphi_2\omega_2-b\sin\varphi_3\omega_3)\cos\varphi_4\omega_4\end{cases} \quad (47)$$

$$\begin{cases}\varepsilon_6 \cdot g= \\ =(\ddot{x}_A-\ddot{x}_E+a\cos\varphi_2\omega_2^2+a\sin\varphi_2\varepsilon_2+c\cos\varphi_3\omega_3^2+c\sin\varphi_3\varepsilon_3)\sin\varphi_6+ \\ (\dot{x}_A-\dot{x}_E+a\sin\varphi_2\omega_2+c\sin\varphi_3\omega_3)\cos\varphi_6\omega_6+\cos\varphi_6(\ddot{y}_E-\ddot{y}_A-a\sin\varphi_2\omega_2^2+ \\ a\cos\varphi_2\varepsilon_2-c\sin\varphi_3\omega_3^2+c\cos\varphi_3\varepsilon_3)-(\dot{y}_E-\dot{y}_A+a\cos\varphi_2\omega_2+c\cos\varphi_3\omega_3)\sin\varphi_6\omega_6\end{cases} \quad (48)$$

$$\begin{cases}\ddot{x}_C=-d\cdot\cos\varphi_4\cdot\omega_4^2-d\cdot\sin\varphi_4\cdot\varepsilon_4 \\ \ddot{y}_C=-d\cdot\sin\varphi_4\cdot\omega_4^2+d\cdot\cos\varphi_4\cdot\varepsilon_4\end{cases} \quad (49)$$

$$\begin{cases}\ddot{x}_B=\ddot{x}_A+a\cdot\cos\varphi_2\cdot\omega_2^2+a\cdot\sin\varphi_2\cdot\varepsilon_2 \\ \ddot{y}_B=\ddot{y}_A+a\cdot\sin\varphi_2\cdot\omega_2^2-a\cdot\cos\varphi_2\cdot\varepsilon_2\end{cases} \quad (50)$$

$$\begin{cases}\ddot{x}_D=\ddot{x}_E+g\cdot\cos\varphi_6\cdot\omega_6^2+g\cdot\sin\varphi_6\cdot\varepsilon_6 \\ \ddot{y}_D=\ddot{y}_E+g\cdot\sin\varphi_6\cdot\omega_6^2-g\cdot\cos\varphi_6\cdot\varepsilon_6\end{cases} \quad (51)$$

$$\begin{cases}\ddot{x}_T=\ddot{x}_D+h\cdot\cos\varphi_6\cdot\omega_6^2+h\cdot\sin\varphi_6\cdot\varepsilon_6 \\ \ddot{y}_T=\ddot{y}_D+h\cdot\sin\varphi_6\cdot\omega_6^2-h\cdot\cos\varphi_6\cdot\varepsilon_6\end{cases} \quad (52)$$

3. RESULTS AND DISCUSSION

Table 1 gives the input data, more precisely the known lengths of the mechanism (In the calculation program used these lengths represent the constant geometric parameters):

Table 1: Constant geometric parameters

XA	0.1	ET	1.35
XG	-0.15	OF	0.15
AB	1.15	FG	0.45
CD	0.88	TD	0.9
OE	0.88	BD	0.7
OC	0.45	BC	0.18
ED	0.45		

INDEPENDENT JOURNAL OF MANAGEMENT & PRODUCTION (IJM&P)
http://www.ijmp.jor.br v. 12, n. 9, Special Edition, December 21, IFLOG 2020
ISSN: 2236-269X
DOI: 10.14807/ijmp.v12i9.1554

The point T located on the effector 6 (Figure 1, 4-5) describes a rectangular trajectory (Figure 12). Its characteristics are shown in Table 2.

Table 2: Initial parameters of the T point trajectory

Initial parameters of the T point	T0(1.5,-0.9)
The step of moving the T point horizontally - v	-0.05
The step of moving the T point vertically - v1	0.05

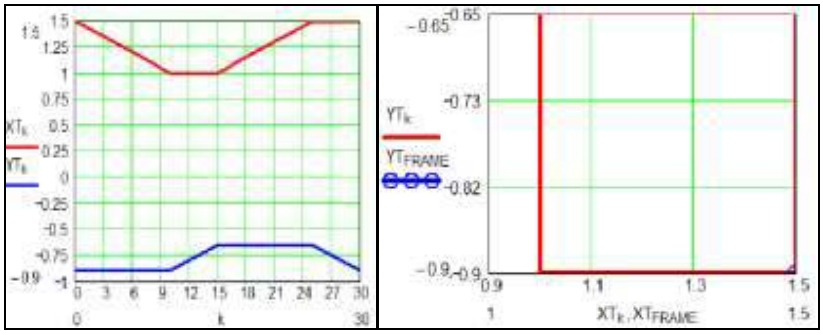

Figure 12: The trajectory of the T-point, the end effector

The trajectory of the point T in Figure 12 is described by the relationships in Table 3.

The coordinates represent the input parameters for the algorithm of the inverse positional model in Table 3.

Table 3: The input parameters

Point T coordinates	*XTk =if [k ≤10,XT0+ kv,if [10< k≤ 15,XT0+ 10v,if[15<k ≤25,XT0+10v-(k-15)v,XT0]]]* *YTk=if [k ≤10,YT0,if[10<k≤15,YT0+(k-10)v1,* *if [15< k ≤25,YT0+ 5v1,YT0 +5v1- (k - 25)v1]]]*

Going through the connection of the modular groups for the inverse structural model (Figure 2b, 3) the algorithm presented in Tables 2-3 allows the successive calculation of the dependent parameters (Figure 4), as follows: - for the dyad RRR(5,6) - Φ5k(XTk,YTk), Φ6k(XTk,YTk) can be seen in Figure 13 [deg], as Φ50k(XTk,YTk), Φ60k(XTk,YTk);

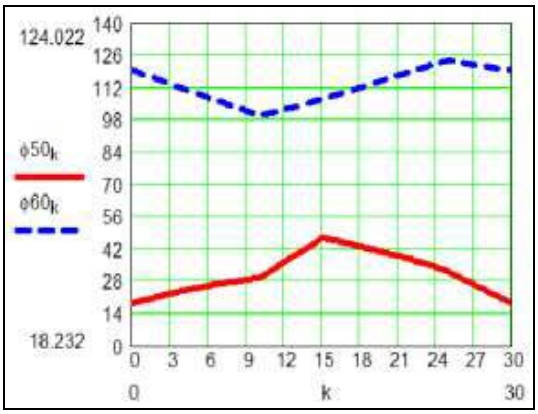

Figure 13: Variation of angles FI5 and FI6 considered in [deg] depending on the independent parameter k

ISSN: 2236-269X
DOI: 10.14807/ijmp.v12i9.1554

- for the dyad RRR(3,4) – Φ3k(XTk,YTk), Φ4k(XTk,YTk) can be seen in the Figure 14 [deg], as Φ30k(XTk,YTk), Φ40k(XTk,YTk);

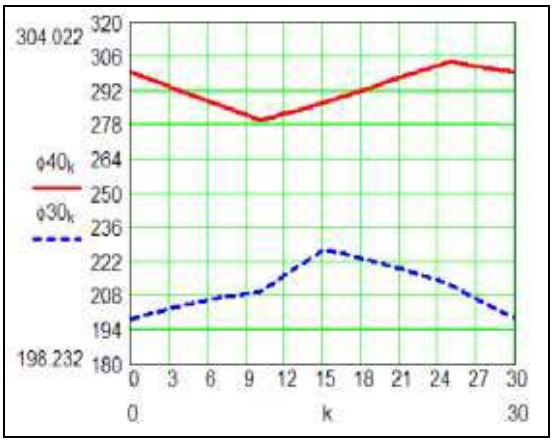

Figure 14: Variation of angles FI3 and FI4 considered in [deg] depending on the independent parameter k

- for dyad RRT(1,2) – YAk(XTk,YTk) and Φ2k(XTk,YTk) seen in Figure 15, where
- Φ2k(XTk,YTk) in [deg] is Φ20k(XTk,YTk);

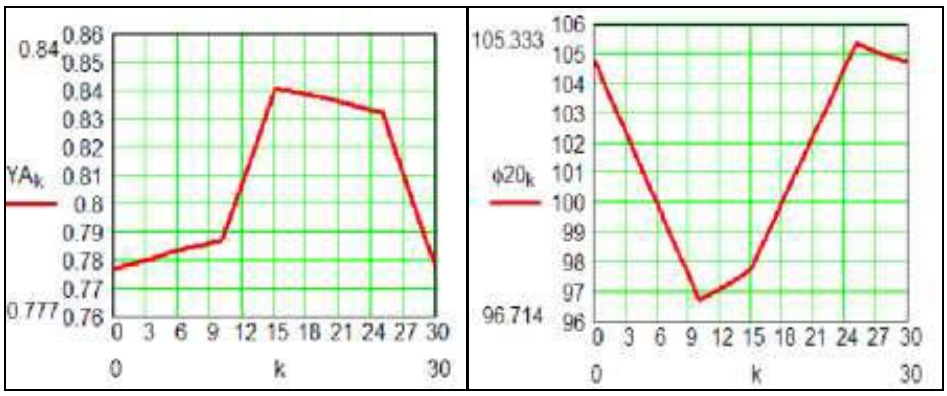

Figure 15: The variation of the parameter YA and the angle FI2 considered in [deg] depending on the independent parameter k

- for dyad RRT(8,7) – YGk(XTk,YTk) and Φ7k(XTk,YTk) seen in Figure 16, where
- Φ7k(XTk,YTk) in [deg] is Φ70k(XTk,YTk).

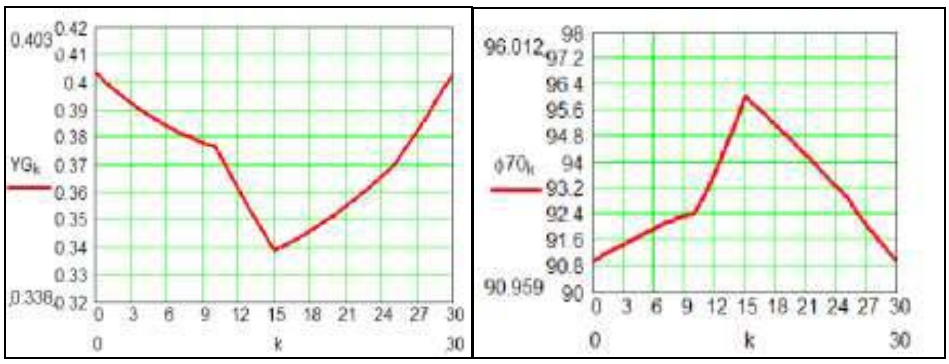

Figure 16: Variation of parameter YG and angle FI7 considered in [deg] depending on the independent parameter k

INDEPENDENT JOURNAL OF MANAGEMENT & PRODUCTION (IJM&P)
http://www.ijmp.jor.br v. 12, n. 9, Special Edition, December 21, IFLOG 2020
ISSN: 2236-269X
DOI: 10.14807/ijmp.v12i9.1554

It is considered a single external force (technological resistance) RTk that acts on the system neglecting other external forces (for example - gravitational forces) and the system of inertial forces. This simplification brings some peculiarities in the form of terms from the calculation algorithm without restricting its generality.

The external force RTk (Figure 17) is considered constant on the initial and horizontal portion of the trajectory of the point T (Figure 12) and is described by the relation (53):

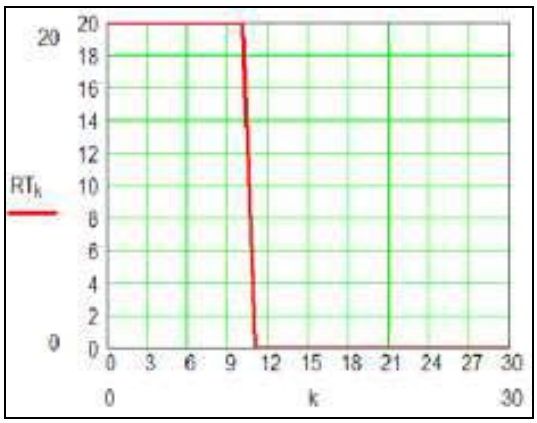

Figure 17: The external force RTk is considered constant on the initial and horizontal portion of the trajectory of the point T

$$RTk := \text{if}(k \leq 10, 20, 0) \quad (53)$$

Using the connection of the modular groups for the direct structural model (Figure 3) the passive module GMP2 (2,3,4,6), a 6R triad (Figure 5, 6, 18) is analyzed in a first stage, for which elaborated algorithm, relations (1-20).

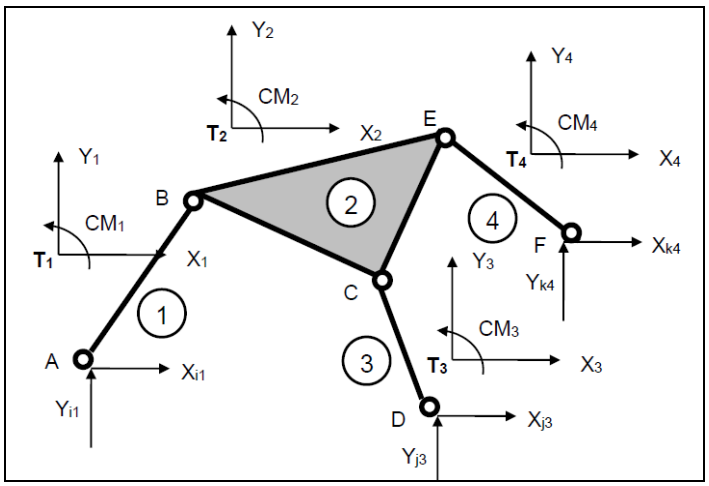

Figure 18: Passive module GMP2(2,3,4,6), the triad 6R

Applying the calculation algorithm (1-20) for the GMP2 triad (2,3,4,6) is determined reaction torsion components, as follows:

- in the kinematic torque of E → X56k, Y56k from Figure 19;

INDEPENDENT JOURNAL OF MANAGEMENT & PRODUCTION (IJM&P)
http://www.ijmp.jor.br v. 12, n. 9, Special Edition, December 21, IFLOG 2020
ISSN: 2236-269X
DOI: 10.14807/ijmp.v12i9.1554

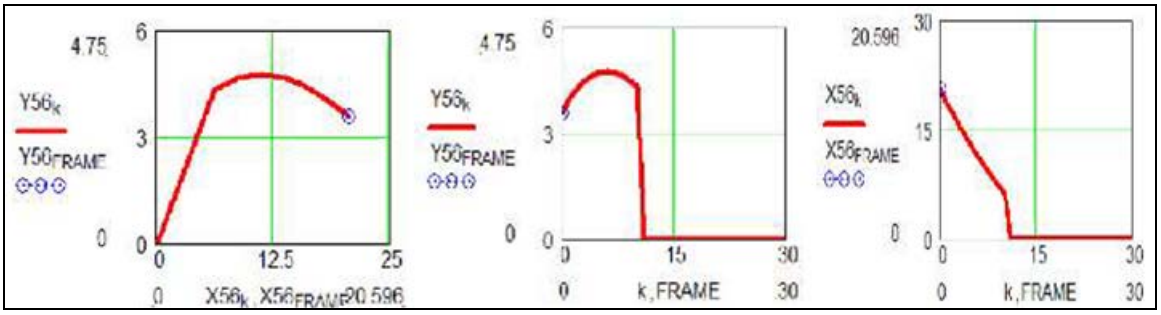

Figure 19: Reaction torque in the kinematic rotation coupling of E → X56k, Y56k on the GMP2 modular group (2,3,4,6), triad type 6R

- in kinematic rotation couple from the point A → X12k, Y12k from Figure 20;

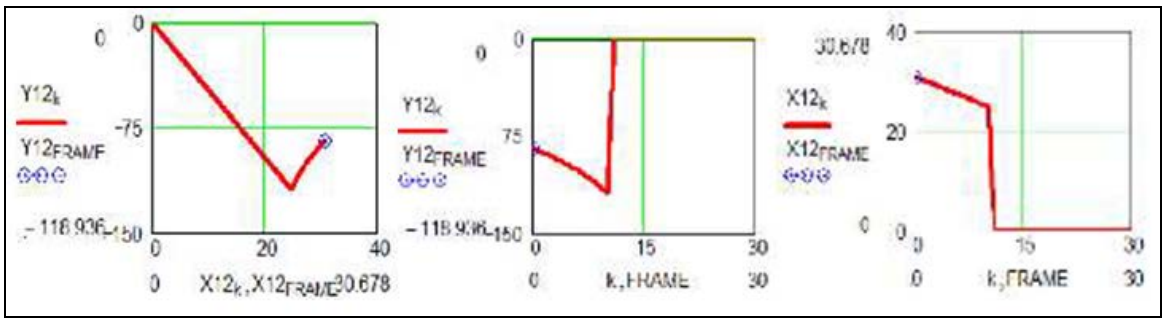

Figure 20: Reaction torque in the kinematic torque of A → X12k, Y12k on the GMP2 modular group (2,3,4,6), 6R triad type

- in the kinematic rotation couple from the point B → X23k = -X32k, Y23k = -Y32k;
- in the kinematic rotation couple from the point C → X43k =-X34k, Y43k =-Y34k;
- in the kinematic rotation couple from the point D → X63k=-X36k, Y63k=-Y36k;
- in the kinematic rotation couple from the point O → X04k, Y04k from Figure 21;

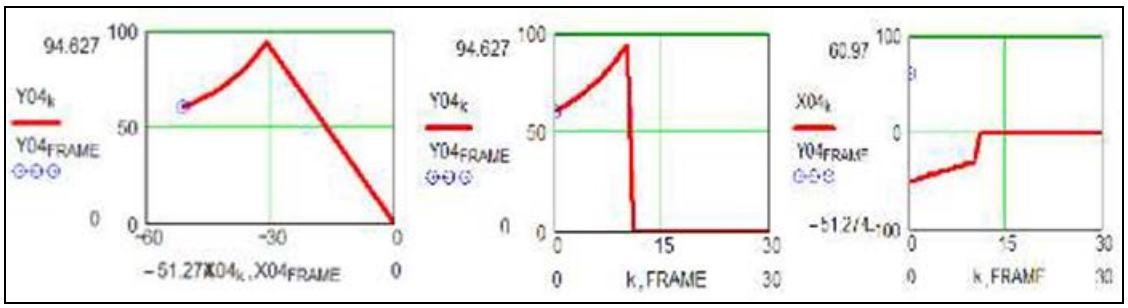

Figure 21: Reaction torsion in the kinematic torque of O → X04k, Y04k on the GMP2 modular group (2,3,4,6), triad type 6R

The next module in the modular group connection of the direct structural model (Figure 7) is GMP1 (7.5) shown in Figure 22 a, b, an RRR dyad for which the kinetostatic model is rendered by the relations (21-32).

INDEPENDENT JOURNAL OF MANAGEMENT & PRODUCTION (IJM&P)
http://www.ijmp.jor.br v. 12, n. 9, Special Edition, December 21, IFLOG 2020
ISSN: 2236-269X
DOI: 10.14807/ijmp.v12i9.1554

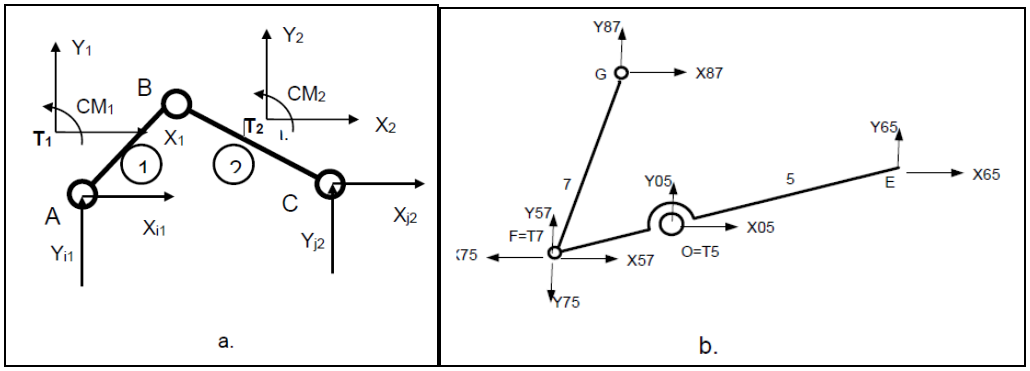

Figure 22: Reaction torsor on the GMP1 dyad modular group (7.5)

In this calculation stage it is determined:

- in the kinematic torque from E → X87k, Y87k from Figure 2. 3;

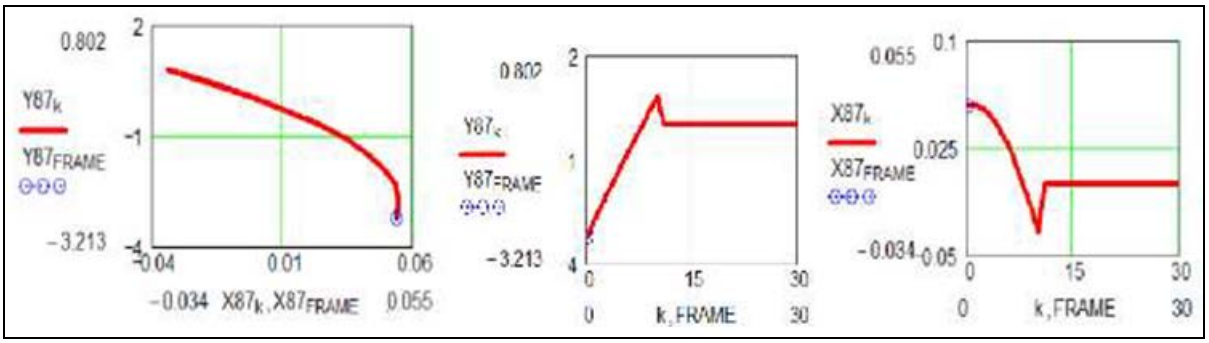

Figure 23: Reaction torsor in kinematic coupling E, → X87k, Y87k, on the GMP1 dyad modular group (7.5)

- in the kinematic rotation couple from the point O → X05k, Y05k from Figure 24.

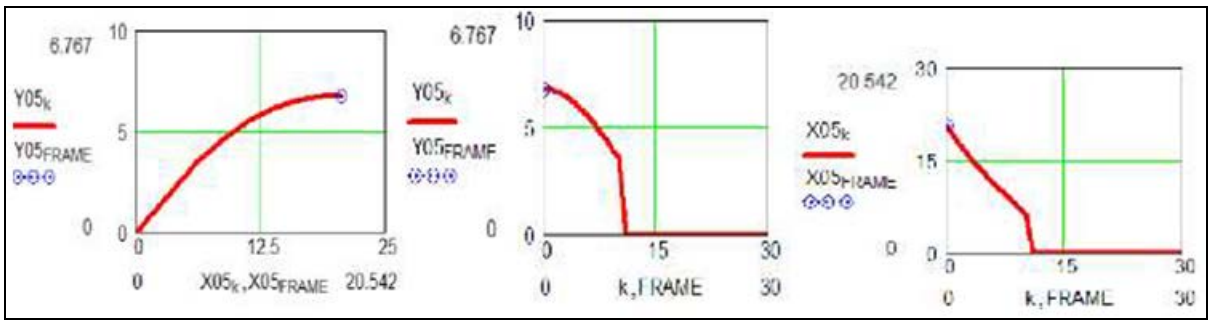

Figure 24: Reaction torsor in kinematic coupling O, → X05k, Y05k, from the GMP1 dyad modular group (7.5)

In the following steps, the initial active modular groups GMAI (G, 8) and GMAI (A, 1) shown in Figs. 25 a, b.

INDEPENDENT JOURNAL OF MANAGEMENT & PRODUCTION (IJM&P)
http://www.ijmp.jor.br v. 12, n. 9, Special Edition, December 21, IFLOG 2020
ISSN: 2236-269X
DOI: 10.14807/ijmp.v12i9.1554

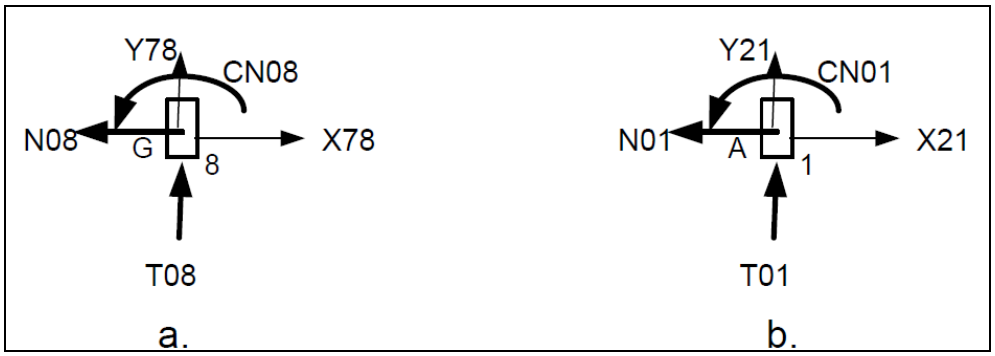

Figure 25: The reaction torsor of the initial active modular groups GMAI (G, 8) a, and GMAI (A, 1) b

The components (NO8k, T08k) of the active translation coupling G are shown in Figs. 26, and for the active coupling of A (NO1k, T01k) in Figs. 27.

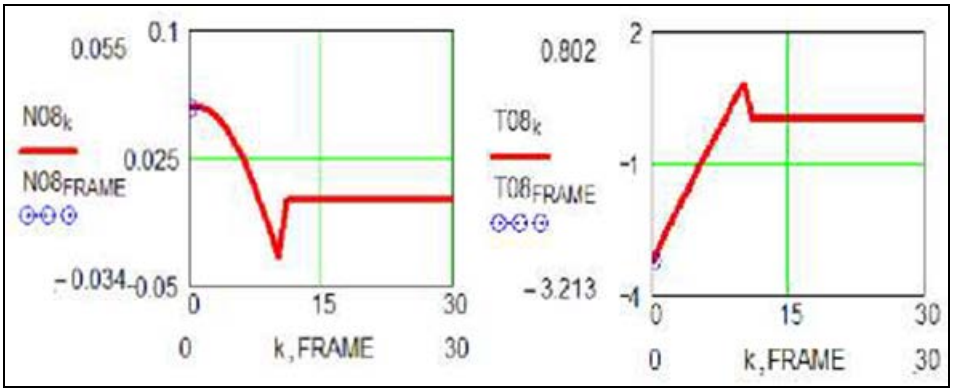

Figure 26: Reaction torsor from the initial active modular group GMAI (G, 8)

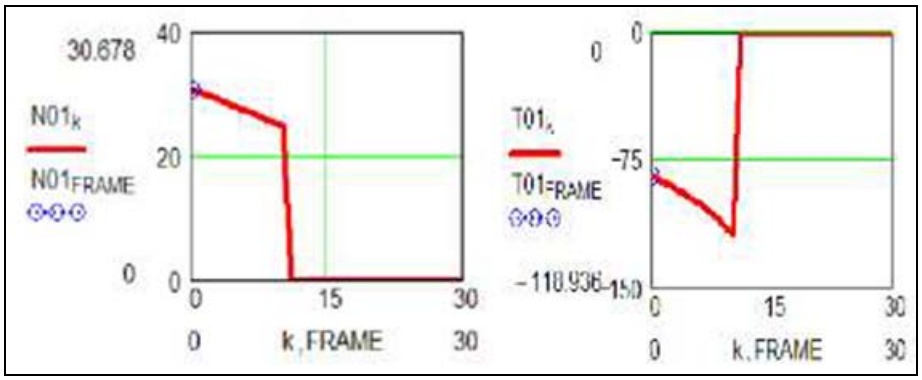

Figure 27: Reaction torsor from the initial active modular group GMAI (A,1)

This bimobile 2T9R mechanism (Figure 1) can be used by the simultaneous action of active translation torques in A and G point T having a chosen trajectory and law of motion. If one of these active couplings is locked, the mechanism remains with only one degree of mobility. The connections of the modular groups are given in both cases: respectively, for G blocked and for A blocked in Figs. 28 a, b.

ISSN: 2236-269X
DOI: 10.14807/ijmp.v12i9.1554

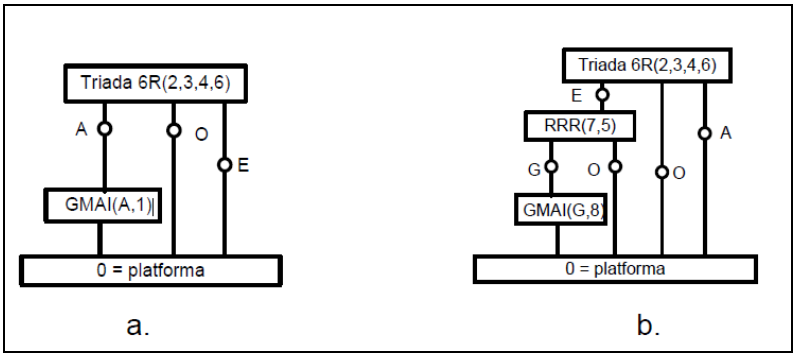

Figure 28: The connections of the modular groups for the two distinct situations when G is blocked and the case when A is blocked, respectively

Applying the calculation modules it is possible to study the behavior of the mechanism with a degree of mobility in the mentioned situations. Thus, if the active coupling G is blocked, the variation of the dependent parameters of the resulting mechanism is studied, with a degree of mobility (Figure 29) for the extreme blocking positions Φ50 minimum and Φ50 maximum.

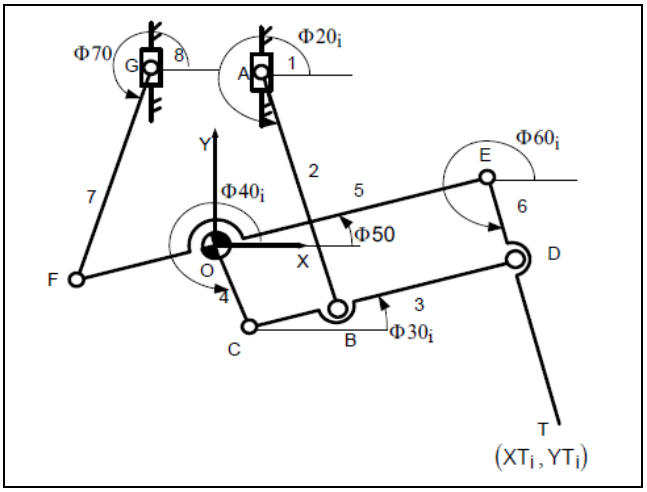

Figure 29: The case in which the active coupling G is blocked when studying the variation of the dependent parameters of the resulting mechanism, with a degree of mobility for the extreme locking positions Φ50 minimum and Φ50 maximum.

4. CONCLUSIONS

The kinematic and kinetostatic modeling of a 2T9R robotic mechanism is generally quite difficult and lucrative, but it has the advantages of obtaining a well-developed theoretical model that can be used in practice to design or use such robots, extremely interesting and useful, which have increased maneuverability, a large workspace, a correct and fast dynamics of movement, without vibrations or noises, the mechatronic module presented can be designed and built-in various ways depending on the requirements and objectives of the workplace in which it will be implemented.

http://www.ijmp.jor.br v. 12, n. 9, Special Edition, December 21, IFLOG 2020
ISSN: 2236-269X
DOI: 10.14807/ijmp.v12i9.1554

The paper presented the inverse and direct kinematic models, the kinetostatic (forces) model that is always studied inversely, together with the related calculation relations.

In the results and discussions section, the diagrams obtained by calculation using the MathCad 2000 program were actually presented.

5. ACKNOWLEDGEMENT

This text was acknowledged and appreciated by Dr. Veturia CHIROIU Honorific member of Technical Sciences Academy of Romania (ASTR) PhD supervisor in Mechanical Engineering.

6. FUNDING INFORMATION

a) 1-Research contract: 1-Research contract: Contract number 36-5-4D/1986 from 24IV1985, beneficiary CNST RO (Romanian National Center for Science and Technology) Improving dynamic mechanisms.

b) 2-Contract research integration. 19-91-3 from 29.03.1991; Beneficiary: MIS; TOPIC: Research on designing mechanisms with bars, cams and gears, with application in industrial robots.

c) 3-Contract research. GR 69/10.05.2007: NURC in 2762; theme 8: Dynamic analysis of mechanisms and manipulators with bars and gears.

d) 4-Labor contract, no. 35/22.01.2013, the UPB, "Stand for reading performance parameters of kinematics and dynamic mechanisms, using inductive and incremental encoders, to a Mitsubishi Mechatronic System" "PN-II-IN-CI-2012-1-0389".

e) All these matters are copyrighted! Copyrights: 394-qodGnhhtej, from 17-02-2010 13:42:18; 463-vpstuCGsiy, from 20-03-2010 12:45:30; 631-sqfsgqvutm, from 24-05-2010 16:15:22; 933-CrDztEfqow, from 07-01-2011 13:37:52.

7. ETHICS

Authors should address any ethical issues that may arise after the publication of this manuscript.

REFERENCES

Antonescu, P., & Petrescu, F. I. T. (1985). An analytical method of synthesis of cam mechanism and flat stick. **Proceedings of the 4th International Symposium on Theory and Practice of Mechanisms**, (TPM’ 89)., Bucharest.

http://www.ijmp.jor.br v. 12, n. 9, Special Edition, December 21, IFLOG 2020
ISSN: 2236-269X
DOI: 10.14807/ijmp.v12i9.1554

Antonescu, P., & Petrescu, F. I. T. (1989). Contributions to kinetoplast dynamic analysis of distribution mechanisms. **SYROM'89**, Bucharest.

Antonescu, P., Oprean, M., & Petrescu, F. I. T. (1985a). Contributions to the synthesis of oscillating cam mechanism and oscillating flat stick. **Proceedings of the 4th International Symposium on Theory and Practice of Mechanisms**, (TPM' 85)., Bucharest.

Antonescu, P., Oprean, M., & Petrescu, F. I. T. (1985b). At the projection of the oscillate cams, there are mechanisms and distribution variables. **Proceedings of the 5th Conference of Engines, Automobiles, Tractors and Agricultural Machines**, (TAM' 58)., I-Motors and Cars, Brasov.

Antonescu, P., Oprean, M., & Petrescu, F. I. T. (1986). Projection of the profile of the rotating camshaft acting on the oscillating plate with disengagement. **Proceedings of the 3rd National Computer-aided Design Symposium in the field of Mechanisms and Machine Parts**, (MMP' 86)., Brasov.

Antonescu, P., Oprean, M., & Petrescu, F. I. T. (1987). Dynamic analysis of the cam distribution mechanisms. **Proceedings of the 7th National Symposium on Industrial Robots and Space Mechanisms**, (RSM' 87)., Bucharest.

Antonescu, P., Oprean, M., & Petrescu, F. I. T. (1988). **Analytical synthesis of Kurz profile**, rotating the flat cam. Mach, Build. Rev.

Antonescu, P., Petrescu, F. I. T., & Antonescu, O. (1994). **Contributions to the synthesis of the rotating cam mechanism and the tip of the balancing tip**. Brasov.

Antonescu, P., Petrescu, F. I. T., & Antonescu, O. (1997). Geometrical synthesis of the rotary cam and balance tappet mechanism. Bucharest, 3, 23-23.

Antonescu, P., Petrescu, F. I. T., & Antonescu, O. (2000ª). Contributions to the synthesis of the rotary disc-cam profile. **Proceedings of the 8th International Conference on the Theory of Machines and Mechanisms**, (TMM' 00)., Liberec, Czech Republic, 51-56.

Antonescu, P., Petrescu, F. I. T., & Antonescu, O. (2000b). Synthesis of the rotary cam profile with balance follower. **Proceedings of the 8th Symposium on Mechanisms and Mechanical Transmissions**, (MMT' 00)., Timişoara, 39-44.

Antonescu, P., Petrescu, F. I. T., & Antonescu, O. (2001). Contributions to the synthesis of mechanisms with rotary disc-cam. **Proceedings of the 8th IFToMM International Symposium on Theory of Machines and Mechanisms**, (TMM' 01)., Bucharest, ROMANIA, 31-36.

Atefi, G., Abdous, M. A., & Ganjehkaviri, A. (2008). Analytical Solution of Temperature Field in Hollow Cylinder under Time Dependent Boundary Condition Using Fourier series, **Am. J. Eng. Applied Sci.**, 1(2), 141-148. DOI: 10.3844/ajeassp.2008.141.148

Avaei, A., Ghotbi, A. R., & Aryafar, M. (2008). Investigation of Pile-Soil Interaction Subjected to Lateral Loads in Layered Soils, **Am. J. Eng. Applied Sci.**, 1(1), 76-81. DOI: 10.3844/ajeassp.2008.76.81

Aversa, R., Petrescu, R. V. V., Apicella, A., & Petrescu, F. I. T. (2017a). Nano-diamond hybrid materials for structural biomedical application. **Am. J. Biochem. Biotechnol.** (13), 34-41. DOI: 10.3844/ajbbsp.2017.34.41

Aversa, R., Petrescu, R. V. V., Akash, B., Bucinell, R. B., & Corchado, J. M. (2017b). Kinematics and forces to a new model forging manipulator. **Am. J. Applied Sci.** (14), 60-80. DOI: 10.3844/ajassp.2017.60.80

http://www.ijmp.jor.br v. 12, n. 9, Special Edition, December 21, IFLOG 2020
ISSN: 2236-269X
DOI: 10.14807/ijmp.v12i9.1554

Aversa, R., Petrescu, R. V. V., Apicella, A., Petrescu, F. I. T., & Calautit, J. K. (2017c). Something about the V engines design. **Am. J. Applied Sci.** (14), 34-52. DOI: 10.3844/ajassp.2017.34.52

Aversa, R., Parcesepe, D., Petrescu, R. V. V., Berto, F., & Chen, G. (2017d). Process ability of bulk metallic glasses. **Am. J. Applied Sci.** (14), 294-301. DOI: 10.3844/ajassp.2017.294.301

Aversa, R., Petrescu, R. V. V., Akash, B., Bucinell, R. B., & Corchado, J. M. (2017e). Something about the balancing of thermal motors. **Am. J. Eng. Applied Sci. (**10), 200-217. DOI: 10.3844/ajeassp.2017.200.217

Aversa, R., Petrescu, F. I. T., Petrescu, R. V. V., & Apicella, A. (2016a). Biomimetic FEA bone modeling for customized hybrid biological prostheses development. **Am. J. Applied Sci. (**13), 1060-1067. DOI: 10.3844/ajassp.2016.1060.1067

Aversa, R., Parcesepe, D., Petrescu, R. V. V., Chen, G., & PETRESCU, F. I. T. (2016b). Glassy amorphous metal injection molded induced morphological defects. **Am. J. Applied Sci. (**13), 1476-1482. DOI: 10.3844/ajassp.2016.1476.1482

Aversa, R., Petrescu, R. V. V., Petrescu, F. I. T., & Apicella, A., (2016c). Smart-factory: Optimization and process control of composite centrifuged pipes. **Am. J. Applied Sci.** (13), 1330-1341. DOI: 10.3844/ajassp.2016.1330.1341

Aversa, R., Tamburrino, F., Petrescu, R. V. V., Petrescu, F. I. T., & Artur, M. (2016d). Biomechanically inspired shape memory effect machines driven by muscle like acting NiTi alloys. **Am. J. Applied Sci.** (13), 1264-1271. DOI: 10.3844/ajassp.2016.1264.1271

Aversa, R., Buzea, E. M., Petrescu, R. V. V., Apicella, A., & Neacsa, M. (2016e). Present a mechatronic system having able to determine the concentration of carotenoids. **Am. J. Eng. Applied Sci.** (9), 1106-1111. DOI: 10.3844/ajeassp.2016.1106.1111

Aversa, R., Petrescu, R. V. V., Sorrentino, R., Petrescu, F. I. T., & Apicella, A. (2016f). Hybrid ceramo-polymeric nanocomposite for biomimetic scaffolds design and preparation. **Am. J. Eng. Applied Sci.** (9), 1096-1105. DOI: 10.3844/ajeassp.2016.1096.1105

Aversa, R., Perrotta, Petrescu, R. V. V., Misiano, C., & Petrescu, F. I. T. (2016g). From structural colors to super-hydrophobicity and achromatic transparent protective coatings: Ion plating plasma assisted TiO_2 and SiO_2 nano-film deposition. **Am. J. Eng. Applied Sci.** (9), 1037-1045. DOI: 10.3844/ajeassp.2016.1037.1045

Aversa, R., Petrescu, R. V. V., Petrescu, F. I. T., & Apicella, A. (2016h).. Biomimetic and evolutionary design driven innovation in sustainable products development. **Am. J. Eng. Applied Sci.** (9), 1027-1036. DOI: 10.3844/ajeassp.2016.1027.1036

Aversa, R., Petrescu, R. V. V., Apicella, A., & Petrescu, F. I. T. (2016i). Mitochondria are naturally micro robots - a review. **Am. J. Eng. Applied Sci.**, (9) 991-1002. DOI: 10.3844/ajeassp.2016.991.1002

Aversa, R., Petrescu, R. V. V., Apicella, A., & Petrescu, F. I. T. (2016j). We are addicted to vitamins C and E-A review. **Am. J. Eng. Applied Sci.** (9), 1003-1018. DOI: 10.3844/ajeassp.2016.1003.1018

Aversa, R., Petrescu, R. V. V., Apicella, A., & Petrescu, F. I. T. (2016k). Physiologic human fluids and swelling behavior of hydrophilic biocompatible hybrid ceramo-polymeric materials. **Am. J. Eng. Applied Sci.** (9), 962-972. DOI: 10.3844/ajeassp.2016.962.972

ISSN: 2236-269X
DOI: 10.14807/ijmp.v12i9.1554

Aversa, R., Petrescu, R. V. V., Apicella, A., & Petrescu, F. I. T. (2016l). One can slow down the aging through antioxidants. **Am. J. Eng. Applied Sci.** (9), 1112-1126. DOI: 10.3844/ajeassp.2016.1112.1126

Aversa, R., Petrescu, R. V. V., Apicella, A., & Petrescu, F. I. T. (2016m). About homeopathy or ≪Similia Similibus Curentur≫. **Am. J. Eng. Applied Sci.** (9), 1164-1172. DOI: 10.3844/ajeassp.2016.1164.1172

Aversa, R., Petrescu, R. V. V., Apicella, A., & Petrescu, F. I. T. (2016n). The basic elements of life's. **Am. J. Eng. Applied Sci.** (9), 1189-1197. DOI: 10.3844/ajeassp.2016.1189.1197

Aversa, R., Petrescu, F. I. T., Petrescu, R. V. V., & Apicella, A. (2016o). Flexible stem trabecular prostheses. **Am. J. Eng. Applied Sci.** (9), 1213-1221. DOI: 10.3844/ajeassp.2016.1213.122

Azaga, M., & Othman, M. (2008). Source Couple Logic (SCL).: Theory and Physical Design, **Am. J. Eng. Applied Sci.**, 1(1), 24-32. DOI: 10.3844/ajeassp.2008.24.32

Cao, W., Ding, H., Bin, Z., & Ziming, C. (2013). New structural representation and digital-analysis platform for symmetrical parallel mechanisms. **Int. J. Adv. Robotic Sys**. DOI: 10.5772/56380

Comanescu, A. (2010). Bazele Modelarii Mecanismelor. 1st Edn., **E. Politeh, Press**, Bucureşti, 274.

Dong, H., Giakoumidis, N., Figueroa, N., & Mavridis, N. (2013). Approaching behaviour monitor and vibration indication in developing a General Moving Object Alarm System (GMOAS).. **Int. J. Adv. Robotic Sys**. DOI: 10.5772/56586

Yousif El-Tous, (2008). Pitch Angle Control of Variable Speed Wind Turbine, **Am. J. Eng. Applied Sci.**, 1(2), 118-120. DOI: 10.3844/ajeassp.2008.118.120

Franklin, D. J. (1930). Ingenious Mechanisms for Designers and Inventors. 1st Edn., **Industrial Press Publisher**.

He, B., Wang, Z., Li, Q., Xie, H., & Shen, R. (2013). An analytic method for the kinematics and dynamics of a multiple-backbone continuum robot. **IJARS**. DOI: 10.5772/54051

Jolgaf, M., Sulaiman, S. B., Ariffin, M. K. A., & Faieza, A. A. (2008). Closed Die Forging Geometrical Parameters Optimization for Al-MMC, **Am. J. Eng. Applied Sci.**, 1(1), 1-6. DOI : 10.3844/ajeassp.2008.1.6

Kannappan, A. N., Kesavasamy, R., & Ponnuswamy, V. (2008). Molecular Interaction Studies of H-Bonded Complexes of Benzamide in 1,4-Dioxan with Alcohols From Acoustic and Thermodynamic Parameters, **Am. J. Eng. Applied Sci.**, 1(2), 95-99. DOI: 10.3844/ajeassp.2008.95.99

Lee, B. J. (2013). Geometrical derivation of differential kinematics to calibrate model parameters of flexible manipulator. **Int. J. Adv. Robotic Sys**. DOI: 10.5772/55592

Lin, W., Li, B., Yang, X., & Zhang, D. (2013). Modelling and control of inverse dynamics for a 5-DOF parallel kinematic polishing machine. **Int. J. Adv. Robotic Sys**. DOI: 10.5772/54966

Liu, H., Zhou, W., Lai, X., & Zhu, S. (2013). An efficient inverse kinematic algorithm for a PUMA560-structured robot manipulator. **IJARS**. DOI: 10.5772/56403

ISSN: 2236-269X
DOI: 10.14807/ijmp.v12i9.1554

Meena, P., & Rittidech, S. (2008). Comparisons of Heat Transfer Performance of a Closed-looped Oscillating Heat Pipe and Closed-looped Oscillating Heat Pipe with Check Valves Heat Exchangers, **Am. J. Eng. Applied Sci**., 1(1), 7-11. DOI: 10.3844/ajeassp.2008.7.11

Meena, P., Rittidech, S., & Tammasaeng, P. (2008). Effect of Inner Diameter and Inclination Angles on Operation Limit of Closed-Loop Oscillating Heat-Pipes with Check Valves, **Am. J. Eng. Applied Sci.**, 1(2), 100-103. DOI: 10.3844/ajeassp.2008.100.103

Mirsayar, M. M., Joneidi, A., Petrescu, R. V. V., Petrescu, F. I. T., & Berto, F. (2017). Extended MTSN criterion for fracture analysis of soda lime glass. **Eng. Fracture Mechan. (**178), 50-59. DOI: 10.1016/j.engfracmech.2017.04.018

Ng, K. C., Yusoff,M. Z., Munisamy, K., Hasini, H., & Shuaib, N. H. (2008). Time-Marching Method for Computations of High-Speed Compressible Flow on Structured and Unstructured Grid, **Am. J. Eng. Applied Sci.**, 1(2), 89-94. DOI: 10.3844/ajeassp.2008.89.94

Padula, F., & Perdereau, V. (2013). An on-line path planner for industrial manipulators. **Int. J. Adv. Robotic Sys**. DOI: 10.5772/55063

Pannirselvam, N., Raghunath, N., & Suguna, K. (2008). Neural Network for Performance of Glass Fibre Reinforced Polymer Plated RC Beams, **Am. J. Eng. Applied Sci.**, 1(1), 82-88. DOI: 10.3844/ajeassp.2008.82.88

Perumaal, S., & Jawahar (2013). Automated trajectory planner of industrial robot for pick-and-place task. **IJARS**. DOI: 10.5772/53940

Petrescu, F. I. T., & Petrescu, R. V. V. (1995a). **Contributions to optimization of the polynomial motion laws of the stick from the internal combustion engine distribution mechanism**. Bucharest(1), 249-256.

Petrescu, F. I. T., & Petrescu, R. V. V. (1995b). **Contributions to the synthesis of internal combustion engine distribution mechanisms**. Bucharest (1), 257-264.

Petrescu, F. I. T., & Petrescu, R. V. V. (1997a). **Dynamics of cam mechanisms (exemplified on the classic distribution mechanism).**. Bucharest (3), 353-358.

Petrescu, F. I. T., & Petrescu, R. V. V. (1997b). **Contributions to the synthesis of the distribution mechanisms of internal combustion engines with a Cartesian coordinate method**. Bucharest (3), 359-364.

Petrescu, F. I. T., & Petrescu, R. V. V. (1997c). **Contributions to maximizing polynomial laws for the active stroke of the distribution mechanism from internal combustion engines**. Bucharest (3), 365-370.

Petrescu, F. I. T., & Petrescu, R. V. V. (2000a). Synthesis of distribution mechanisms by the rectangular (Cartesian). coordinate method. **Proceedings of the 8th National Conference on International Participation**, (CIP' 00)., Craiova, Romania, 297-302.

Petrescu, F. I. T., & Petrescu, R. V. V. (2000b). The design (synthesis). of cams using the polar coordinate method (triangle method).. **Proceedings of the 8th National Conference on International Participation**, (CIP' 00)., Craiova, Romania, 291-296.

Petrescu, F. I. T., & Petrescu, R. V. V. (2002a). Motion laws for cams. Proceedings of the International Computer Assisted Design, **National Symposium Participation**, (SNP' 02)., Braşov, p 321-326.

Petrescu, F. I. T., & Petrescu, R. V. V. (2002b). Camshaft dynamics elements. **Proceedings of the International Computer Assisted Design, National Participation Symposium**, (SNP' 02)., Braşov, 327-332.

ISSN: 2236-269X
DOI: 10.14807/ijmp.v12i9.1554

Petrescu, F. I. T., & Petrescu, R. V. V. (2003). Some elements regarding the improvement of the engine design. **Proceedings of the National Symposium, Descriptive Geometry, Technical Graphics and Design**, (GTD' 03)., Braşov, 353-358.

Petrescu, F. I. T., & Petrescu, R. V. V. (2005a). The cam design for a better efficiency. **Proceedings of the International Conference on Engineering Graphics and Design**, (EGD' 05)., Bucharest, 245-248.

Petrescu, F. I. T., & Petrescu, R. V. V. (2005b). Contributions at the dynamics of cams. **Proceedings of the 9th IFToMM International Symposium on Theory of Machines and Mechanisms**, (TMM' 05)., Bucharest, Romania, 123-128.

Petrescu, F. I. T., & Petrescu, R. V. V. (2005c). Determining the dynamic efficiency of cams. **Proceedings of the 9th IFToMM International Symposium on Theory of Machines and Mechanisms**, (TMM' 05)., Bucharest, Romania, 129-134.

Petrescu, F. I. T., & Petrescu, R. V. V. (2005d). An original internal combustion engine. **Proceedings of the 9th IFToMM International Symposium on Theory of Machines and Mechanisms**, (TMM' 05)., Bucharest, Romania, 135-140.

Petrescu, F. I. T., & Petrescu, R. V. V. (2005e). Determining the mechanical efficiency of Otto engine's mechanism. **Proceedings of the 9th IFToMM International Symposium on Theory of Machines and Mechanisms**, (TMM 05)., Bucharest, Romania, 141-146.

Petrescu, F. I. T., & Petrescu, R. V. V. (2011a). Mechanical Systems, Serial and Parallel (Romanian).. 1st Edn., **LULU Publisher**, London, UK, 124.

Petrescu, F. I. T., & Petrescu, R. V. V. (2011b). Trenuri Planetare. **Createspace Independent Pub**., 104 pages, ISBN-13: 978-1468030419.

Petrescu, F. I. T., & Petrescu, R. V. V. (2012a). Kinematics of the planar quadrilateral mechanism. **ENGEVISTA** (14), 345-348.

Petrescu, F. I. T., & Petrescu, R. V. V. (2012b). Mecatronica-Sisteme Seriale si Paralele. 1st Edn., **Create Space Publisher**, USA, 128.

Petrescu, F. I. T., & Petrescu, R. V. V. (2013a). Cinematics of the 3R dyad. **ENGEVISTA** (15), 118-124.

Petrescu, F. I. T., & Petrescu, R. V. V. (2013b). Forces and efficiency of cams. **Int. Rev. Mechanical Eng**.

Petrescu, F. I. T., & Petrescu, R. V. V. (2016a). Parallel moving mechanical systems kinematics. **ENGEVISTA** (18), 455-491.

Petrescu, F. I. T., & Petrescu, R. V. V. (2016b). Direct and inverse kinematics to the anthropomorphic robots. **ENGEVISTA** (18), 109-124.

Petrescu, F. I. T., & Petrescu, R. V. V. (2016c). Dynamic cinematic to a structure 2R. **Revista Geintec-Gestao Inovacao E Tecnol.** (6), 3143-3154.

Petrescu, F. I. T., Grecu, B., Comanescu, A., & Petrescu, R. V. V. (2009). Some mechanical design elements. **Proceeding of the International Conference on Computational Mechanics and Virtual Engineering**, (MVE' 09)., Braşov, 520-525.

Petrescu, F. I. T. (2011). Teoria Mecanismelor si a Masinilor: Curs Si Aplicatii. 1st Edn., **CreateSpace Independent Publishing Platform**. ISBN-10: 1468015826. 432.

Petrescu, F. I. T. (2015a). Geometrical synthesis of the distribution mechanisms. **Am. J. Eng. Applied Sci.** (8), 63-81. DOI: 10.3844/ajeassp.2015.63.81

http://www.ijmp.jor.br v. 12, n. 9, Special Edition, December 21, IFLOG 2020
ISSN: 2236-269X
DOI: 10.14807/ijmp.v12i9.1554

Petrescu, F. I. T. (2015b). Machine motion equations at the internal combustion heat engines. **Am. J. Eng. Applied Sci.**, (8), 127-137. DOI: 10.3844/ajeassp.2015.127.137

Petrescu, R. V. V., Aversa, R., Apicella, A., & Petrescu, F. I. T. (2016). Future medicine services robotics. **Am. J. Eng. Applied Sci.** (9), 1062-1087. DOI: 10.3844/ajeassp.2016.1062.1087

Petrescu, R. V. V., Aversa, R., Akash, B., Bucinell, R., & Corchado, J. (2017a). Yield at thermal engines internal combustion. **Am. J. Eng. Applied Sci.** (10), 243-251. DOI: 10.3844/ajeassp.2017.243.251

Petrescu, R. V. V., Aversa, R., Akash, B., Ronald, B., & Corchado, J. (2017b). Velocities and accelerations at the 3R mechatronic systems. **Am. J. Eng. Applied Sci.** (10), 252-263. DOI: 10.3844/ajeassp.2017.252.263

Petrescu, R. V. V., Aversa, R., Akash, B., Bucinell, R., & Corchado, J. (2017c). Anthropomorphic solid structures n-r kinematics. **Am. J. Eng. Applied Sci.** (10), 279-291. DOI: 10.3844/ajeassp.2017.279.291

Petrescu, R. V. V., Aversa, R., Akash, B., Bucinell, R., & Corchado, J. (2017d). Inverse kinematics at the anthropomorphic robots, by a trigonometric method. **Am. J. Eng. Applied Sci**. (10), 394-411. DOI: 10.3844/ajeassp.2017.394.411

Petrescu, R. V. V., Aversa, R., Akash, B., Bucinell, R., & Corchado, J. (2017e). Forces at internal combustion engines. **Am. J. Eng. Applied Sci**. (10), 382-393. DOI: 10.3844/ajeassp.2017.382.393

Petrescu, R. V. V., Aversa, R., Akash, B., Bucinell, R., & Corchado, J. (2017f). Gears-Part I. **Am. J. Eng. Applied Sci.** (10), 457-472. DOI: 10.3844/ajeassp.2017.457.472

Petrescu, R. V. V., Aversa, R., Akash, B., Bucinell, R., & Corchado, J. (2017g). Gears-part II. **Am. J. Eng. Applied Sci.** (10), 473-483. DOI: 10.3844/ajeassp.2017.473.483

Petrescu, R. V. V., Aversa, R., Akash, B., Bucinell, R., & Corchado, J. (2017h).. Cam-gears forces, velocities, powers and efficiency. **Am. J. Eng. Applied Sci. (**10), 491-505. DOI: 10.3844/ajeassp.2017.491.505

Petrescu, R. V. V., Aversa, R., Akash, B., Bucinell, R., & Corchado, J. (2017i). Dynamics of mechanisms with cams illustrated in the classical distribution. **Am. J. Eng. Applied Sci. (**10), 551-567. DOI: 10.3844/ajeassp.2017.551.567

Petrescu, R. V. V., Aversa, R., Akash, B., Bucinell, R., & Corchado, J. (2017j). Testing by non-destructive control. **Am. J. Eng. Applied Sci. (**10), 568-583. DOI: 10.3844/ajeassp.2017.568.583

Petrescu, R. V. V., Aversa, R., Apicella, A., & Petrescu, F. I. T., (2017k). Transportation engineering. **Am. J. Eng. Applied Sci. (**10), 685-702. DOI: 10.3844/ajeassp.2017.685.702

Petrescu, R. V. V., Aversa, R., Kozaitis, S., Apicella, A., & Petrescu, F. I. T. (2017l). The quality of transport and environmental protection, part I. **Am. J. Eng. Applied Sci. (**10), 738-755. DOI: 10.3844/ajeassp.2017.738.755

Petrescu, R. V. V., Aversa, R., Akash, B., Bucinell, R., & Corchado, J. (2017m). Modern propulsions for aerospace-a review. J. Aircraft Spacecraft Technol. (1), 1-8. DOI: 10.3844/jastsp.2017.1.8

Petrescu, R. V. V., Aversa, R., Akash, B., Bucinell, R., & Corchado, J. (2017n). Modern propulsions for aerospace-part II. **J. Aircraft Spacecraft Technol. (**1), 9-17. DOI: 10.3844/jastsp.2017.9.17

http://www.ijmp.jor.br v. 12, n. 9, Special Edition, December 21, IFLOG 2020
ISSN: 2236-269X
DOI: 10.14807/ijmp.v12i9.1554

Petrescu, R. V. V., Aversa, R., Akash, B., Bucinell, R., & Corchado, J. (2017o). History of aviation-a short review. **J. Aircraft Spacecraft Technol. (**1), 30-49. DOI: 10.3844/jastsp.2017.30.49

Petrescu, R. V. V., Aversa, R., Akash, B., Bucinell, R., & Corchado, J. (2017p). Lockheed martin-a short review. **J. Aircraft Spacecraft Technol. (**1), 50-68. DOI: 10.3844/jastsp.2017.50.68

Petrescu, R. V. V., Aversa, R., Akash, B., Bucinell, R., & Corchado, J. (2017q). Our universe. **J. Aircraft Spacecraft Technol. (**1), 69-79. DOI: 10.3844/jastsp.2017.69.79

Petrescu, R. V. V., Aversa, R., Akash, B., Corchado, J., & Berto, F. (2017r). What is a UFO? **J. Aircraft Spacecraft Technol. (**1), 80-90. DOI: 10.3844/jastsp.2017.80.90

Petrescu, R. V. V., Aversa, R., Akash, B., Corchado, J., & Berto, F. (2017s). About bell helicopter FCX-001 concept aircraft-a short review. **J. Aircraft Spacecraft Technol. (**1), 91-96. DOI: 10.3844/jastsp.2017.91.96

Petrescu, R. V. V., Aversa, R., Akash, B., Corchado, J., & Berto, F. (2017t). Home at airbus. **J. Aircraft Spacecraft Technol. (**1), 97-118. DOI: 10.3844/jastsp.2017.97.118

Petrescu, R. V. V., Aversa, R., Akash, B., Corchado, J., & Berto, F. (2017u). Airlander. **J. Aircraft Spacecraft Technol. (**1), 119-148. DOI: 10.3844/jastsp.2017.119.148

Petrescu, R. V. V., Ersa, R., Akash, B., Corchado, J., & Berto, F. (2017v). When boeing is dreaming-a review. **J. Aircraft Spacecraft Technol. (**1), 149-161. DOI: 10.3844/jastsp.2017.149.161

Petrescu, R. V. V., Aversa, R., Akash, B., Corchado, J., & Berto, F. (2017w). About Northrop Grumman. **J. Aircraft Spacecraft Technol. (**1), 162-185. DOI: 10.3844/jastsp.2017.162.185

Petrescu, R. V. V., Aversa, R., Akash, B., Corchado, J., & Berto, F. (2017x). Some special aircraft. **J. Aircraft Spacecraft Technol. (**1), 186-203. DOI: 10.3844/jastsp.2017.186.203

Petrescu, R. V. V., Aversa, R., Akash, B., Corchado, J., & Berto, F. (2017y). About helicopters. **J. Aircraft Spacecraft Technol. (**1), 204-223. DOI: 10.3844/jastsp.2017.204.223

Petrescu, R. V. V., Aversa, R., Akash, B., Berto, F., & Apicella, A. (2017z). The modern flight. **J. Aircraft Spacecraft Technol. (**1), 224-233. DOI: 10.3844/jastsp.2017.224.233

Petrescu, R. V. V., Aversa, R., Akash, B., Berto, F., & Apicella, A. (2017aa). Sustainable energy for aerospace vessels. **J. Aircraft Spacecraft Technol. (**1), 234-240. DOI: 10.3844/jastsp.2017.234.240

Petrescu, R. V. V., Aversa, R., Akash, B., Berto, F., & Apicella, A. (2017ab). Unmanned helicopters. **J. Aircraft Spacecraft Technol. (**1), 241-248. DOI: 10.3844/jastsp.2017.241.248

Petrescu, R. V. V., Aversa, R., Akash, B., Berto, F., & Apicella, A. (2017ac). Project HARP. **J. Aircraft Spacecraft Technol. (**1), 249-257. DOI: 10.3844/jastsp.2017.249.257

Petrescu, R. V. V., Aversa, R., Akash, B., Berto, F., & Apicella, A. (2017ad). Presentation of Romanian engineers who contributed to the development of global aeronautics-part I. **J. Aircraft Spacecraft Technol. (**1), 258-271. DOI: 10.3844/jastsp.2017.258.271

http://www.ijmp.jor.br v. 12, n. 9, Special Edition, December 21, IFLOG 2020
ISSN: 2236-269X
DOI: 10.14807/ijmp.v12i9.1554

Petrescu, R. V. V., Aversa, R., Akash, B., Berto, F., & Apicella, A. (2017ae). A first-class ticket to the planet mars, please. **J. Aircraft Spacecraft Technol. (**1), 272-281. DOI: 10.3844/jastsp.2017.272.281

Petrescu, R. V. V., Aversa, R., Apicella, A., Mirsayar, M. M., & Kozaitis, S. (2018a). NASA started a propeller set on board voyager 1 after 37 years of break. **Am. J. Eng. Applied Sci. (**11), 66-77. DOI: 10.3844/ajeassp.2018.66.77

Petrescu, R. V. V., Aversa, R., Apicella, A., Mirsayar, M. M., & Kozaitis, S. (2018b). There is life on mars? **Am. J. Eng. Applied Sci. (**11), 78-91. DOI: 10.3844/ajeassp.2018.78.91

Petrescu, R. V. V., Aversa, R., Apicella, A., & Petrescu, F. I. T. (2018c). Friendly environmental transport. **Am. J. Eng. Applied Sci. (**11), 154-165. DOI: 10.3844/ajeassp.2018.154.165

Petrescu, R. V. V., Aversa, R., Akash, B., Abu-Lebdeh, T. M., & Apicella, A. (2018d). Buses running on gas. **Am. J. Eng. Applied Sci. (**11), 186-201. DOI: 10.3844/ajeassp.2018.186.201

Petrescu, R. V. V., Aversa, R., Akash, B., Abu-Lebdeh, T. M., & Apicella, A. (2018e). Some aspects of the structure of planar mechanisms. **Am. J. Eng. Applied Sci. (**11), 245-259. DOI: 10.3844/ajeassp.2018.245.259

Petrescu, R. V. V., Aversa, R., Abu-Lebdeh, T. M., Apicella, A., & Petrescu, F. I. T. (2018f). The forces of a simple carrier manipulator. **Am. J. Eng. Applied Sci. (**11), 260-272. DOI: 10.3844/ajeassp.2018.260.272

Petrescu, R. V. V., Aversa, R., Abu-Lebdeh, T. M., Apicella, A., & Petrescu, F. I. T. (2018g). The dynamics of the otto engine. **Am. J. Eng. Applied Sci. (**11), 273-287. DOI: 10.3844/ajeassp.2018.273.287

Petrescu, R. V. V., Aversa, R., Abu-Lebdeh, T. M., Apicella, A., & Petrescu, F. I. T. (2018h). NASA satellites help us to quickly detect forest fires. **Am. J. Eng. Applied Sci. (**11), 288-296. DOI: 10.3844/ajeassp.2018.288.296

Petrescu, R. V. V., Aversa, R., Abu-Lebdeh, T. M., Apicella, A., & Petrescu, F. I. T. (2018i). Kinematics of a mechanism with a triad. **Am. J. Eng. Applied Sci. (**11), 297-308. DOI: 10.3844/ajeassp.2018.297.308

Petrescu, R. V. V., Aversa, R., Apicella, A., & Petrescu, F. I. T. (2018j). Romanian engineering "on the wings of the wind". **J. Aircraft Spacecraft Technol. (**2), 1-18. DOI: 10.3844/jastsp.2018.1.18

Petrescu, R. V. V., Aversa, R., Apicella, A., & Petrescu, F. I. T. (2018k). NASA Data used to discover eighth planet circling distant star. **J. Aircraft Spacecraft Technol. (**2), 19-30. DOI: 10.3844/jastsp.2018.19.30

Petrescu, R. V. V., Aversa, R., Apicella, A., & Petrescu, F. I. T. (2018l). NASA has found the most distant black hole. **J. Aircraft Spacecraft Technol**. (2), 31-39. DOI: 10.3844/jastsp.2018.31.39

Petrescu, R. V. V., Aversa, R., Apicella, A., & Petrescu, F. I. T. (2018m). Nasa selects concepts for a new mission to titan, the moon of saturn. **J. Aircraft Spacecraft Technol.**, 2: 40-52. DOI: 10.3844/jastsp.2018.40.52

Petrescu, R. V. V., Aversa, R., Apicella, A., & Petrescu, F. I. T. (2018n). NASA sees first in 2018 the direct proof of ozone hole recovery. **J. Aircraft Spacecraft Technol. (**2), 53-64. DOI: 10.3844/jastsp.2018.53.64

ISSN: 2236-269X
DOI: 10.14807/ijmp.v12i9.1554

Pourmahmoud, N. (2008). Rarefied Gas Flow Modeling inside Rotating Circular Cylinder, **Am. J. Eng. Applied Sci.**, 1(1), 62-65. DOI: 10.3844/ajeassp.2008.62.65

Rajasekaran, A., Raghunath, N., & Suguna, K. (2008). Effect of Confinement on the Axial Performance of Fibre Reinforced Polymer Wrapped RC Column, **Am. J. Eng. Applied Sci.**, 1(2), 110-117. DOI: 10.3844/ajeassp.2008.110.117

Shojaeefard, M. H., Goudarzi, K., Noorpoor, A. R., & Fazelpour, M. (2008). A Study of Thermal Contact using Nonlinear System Identification Models, **Am. J. Eng. Applied Sci.,** 1(1), 16-23. DOI: 10.3844/ajeassp.2008.16.23

Taher, S. A., Hematti, R., & Nemati, M. (2008). Comparison of Different Control Strategies in GA-Based Optimized UPFC Controller in Electric Power Systems, **Am. J. Eng. Applied Sci.**, 1(1), 45-52. DOI: 10.3844/ajeassp.2008.45.52

Tavallaei, M. A., & Tousi, B. (2008). Closed Form Solution to an Optimal Control Problem by Orthogonal Polynomial Expansion, **Am. J. Eng. Applied Sci.**, 1(2), 104-109. DOI: 10.3844/ajeassp.2008.104.109

Theansuwan, W., & Triratanasirichai, K. (2008). Air Blast Freezing of Lime Juice: Effect of Processing Parameters, **Am. J. Eng. Applied Sci.**, 1(1), 33-39. DOI: 10.3844/ajeassp.2008.33.39

Zahedi, S. A., Vaezi, M., & Tolou, N. (2008). Nonlinear Whitham-Broer-Kaup Wave Equation in an Analytical Solution, **Am. J. Eng. Applied Sci.**, 1(2), 161-167. DOI: 10.3844/ajeassp.2008.161.167

Zulkifli, R., Sopian, K., Abdullah, S., & Takriff, M. S. (2008). Effect of Pulsating Circular Hot Air Jet Frequencies on Local and Average Nusselt Number, **Am. J. Eng. Applied Sci.**, 1(1), 57-61. DOI: 10.3844/ajeassp.2008.57.61